



LABORATÓRIO NACIONAL
DE ENGENHARIA CIVIL

DEPARTAMENTO DE ESTRUTURAS
Núcleo de Engenharia Sísmica e Dinâmica
de Estruturas

Proc. 0305/17/15525

LOSS ESTIMATIONS FOR A REFERENCE SITUATION

Application to Lisbon Metropolitan Area

Project LESSLOSS – Risk Mitigation for Earthquakes and
Landslides. Sixth Programme for Research, Technological
Development and Demonstration of European Commission
Contract No.: GOCE-CT-2003-505448

Lisboa • Junho de 2007

I&D ESTRUTURAS

RELATÓRIO 229/2007 – NESDE

**AVALIAÇÃO DE PERDAS PARA UMA SITUAÇÃO DE REFERÊNCIA.
APLICAÇÃO À REGIÃO METROPOLITANA DE LISBOA**

**LOSS ESTIMATES FOR A REFERENCE SITUATION.
APPLICATION TO LISBON METROPOLITAN AREA**

**ESTIMATION DES PERDES POUR UNE SITUATION DE REFERENCE.
APPLICATION A LA REGION METROPOLITAINE DE LISBONNE.**

NOTA PRÉVIA

Este trabalho apresenta a contribuição do Laboratório Nacional de Engenharia Civil (LNEC) para a tarefa 85 do subprojecto SP10, “Earthquake disaster scenario predictions and loss modelling for urban areas”, do projecto integrado Europeu LESSLOSS, “Risk Mitigation for Earthquakes and Landslides”, patrocinado pelo 6º Programa-Quadro Comunitário. O objectivo daquela tarefa era o de avaliar as perdas em consequência de cenários sísmicos pré-definidos, numa situação de referência, ou seja, antes de serem implementadas estratégias de mitigação do risco sísmico envolvendo a diminuição da vulnerabilidade do parque habitacional da região em estudo. Nesta fase do projecto a avaliação de perdas foi efectuada para três casos estudo, as áreas Metropolitanas de Lisboa, Thessaloniki e Istanbul, sendo que a contribuição do LNEC reportou à Área Metropolitana de Lisboa e concelhos limítrofes. A contribuição do LNEC, conjuntamente com as dos restantes parceiros do subprojecto SP10, foi integrada no relatório desenvolvido para a referida tarefa 85. A forma de divulgação deste relatório foi a sua disponibilização no *site* do projecto LESSLOSS, <http://www.lessloss.org/>, pelo que se justifica a publicação da contribuição do LNEC sob a forma de relatório interno deste Laboratório.

INDEX

1. INTRODUCTION.....	1
2. REVISION OF REFERENCE GROUND MOTION EARTHQUAKE SCENARIOS.....	3
2.1. Justification	3
2.2. Seismic action scenarios based on hazard disaggregation	3
2.2.1. Seismic hazard disaggregation methodology.....	3
2.2.2. Revaluating seismic hazard for Mainland Portugal	5
2.2.3. Disaggregation 3D in M-(X, Y).....	7
2.3. Finite fault propagation based on a seismological model	9
2.3.1. Calibrating seismological model.....	9
2.3.2. Upgrading seismological model.....	10
2.3.3. Attenuation laws derived from the seismological model.....	10
2.4. Ground motion maps.....	12
3. REFERENCE LOSS ESTIMATIONS.....	13
3.1. Exposure analysis.....	13
3.1.1. Typological classification	13
3.1.2. Soil classification	18
3.1.3. Exposure analysis by typological and soil classification	20
3.2. Physical damage.....	21
3.3. Human losses.....	22
3.4. Economic losses	22
4. ANALYSIS OF REFERENCE SCENARIOS	23
4.1. Physical damage.....	27
4.2. Human losses.....	27
4.3. Economic losses	27
5. SEISMIC RISK CURVES	29
6. FINAL CONSIDERATIONS	33
7. REFERENCES.....	35
8. ACKNOWLEDGEMENTS	39

INDEX OF FIGURES

Figure 2.1 – Number of earthquakes with magnitude greater than 3.5 for each quadratic bin with 10×10 km; instrumental catalogue (year > 1909) without aftershocks [Sousa & Campos Costa, 2006].	6
Figure 2.2 – Seismic hazard maps for Mainland Portugal for 50, 95, 475, 975 and 5000 return periods. 95 years RP: Lisbon site chosen for a more detailed graphic analysis of disaggregation. 475 years RP: 278 Portuguese counties. 5000 years RP: zoom of MAL region and its 277 parishes.	7
Figure 2.3 – Joint probability distribution or contribution of magnitude (Mag) and distance (X, Y) for 50, 95, 475, 975 and 5000 return periods for Lisbon site.	8
Figure 2.4 – Peak ground acceleration for bedrock (left) and considering soil columns (right) for MAL, for the 50 years return period.	12
Figure 2.5 – Peak ground acceleration for bedrock (left) and considering soil columns (right) for MAL, for the 475 years return period.	12
Figure 3.1 – Distribution of dwellings per typological classes in MAL (data from Censos 2001).	16
Figure 3.2 – Distribution of inhabitants per typological classes in MAL (data from Censos 2001).	17
Figure 3.3 – Soil columns units for MAL [Carvalho et al., 2002].	18
Figure 3.4 – Geographic distribution of ground type for MAL, according to Portuguese version of EC8.	19
Figure 3.5 – Number of dwellings per typological class and ground type.	20
Figure 3.6 – Number of inhabitants per typological class and ground type.	20
Figure 3.7 – Total area [m ²] in MAL per typological class and ground type.	21
Figure 3.8 – Reference situation: maps of severely and completely damaged dwellings. Losses for 475 return periods scenarios.	21
Figure 3.9 – Reference situation: maps of human losses for 475 return period scenario.	22
Figure 3.10 – Reference situation maps of economic losses for 475 return period scenario.	22
Figure 4.1 – Number of Completely Damaged dwellings normalized by exposure in each typological and soil classes; 475 years return period.	23

Figure 4.2 – Number of Completely Damaged dwellings in each typological and soil classes normalized by Completely Damaged dwellings toll; 475 years return period.....	23
Figure 4.3 – Number of deaths normalized by exposure in each typological and soil classes; 475 years return period.....	24
Figure 4.4 - Number of deaths in each typological and soil classes normalized by death toll; 475 years return period.....	24
Figure 4.5 – Lost area normalized by exposure in each typological and soil classes; 475 years return period.	25
Figure 4.6 - Lost area per typological and soil classes; 475 years return period.	25
Figure 4.7 – Economic losses normalized by exposure in each typological and soil classes; 475 years return period.....	26
Figure 4.8 - Economic losses per typological and soil classes; 475 years return period.....	26
Figure 5.1 – Reference situation: seismic risk curves for physical damages in buildings.....	29
Figure 5.2 – Reference situation: seismic risk curves for human losses. FEMA & NIBS [1999] model.	30
Figure 5.3 – Reference situation: seismic risk curves for economic losses measured in terms of percentual (left scale) and absolute (right scale) building lost area.	30
Figure 5.4 – Reference situation: seismic risk curves for economic losses measured in terms of absolute economic losses in millions of Euros (right scale) and as a percentage (left scale) of Portuguese GDP of 2001.	31
Alexandra Carvalho Research Trainee.....	41

INDEX OF TABLES

Table 2.1 – Seismological parameters.....	10
Table 2.2 – Coefficients of the ground motion relations for rock sites	11
Table 3.1 – Typological and floor classes.	13
Table 3.2 – Number of familiar dwellings in MAL, per epoch of construction, structural type and number of floors (Censos 2001).....	14
Table 3.3 – Number of inhabitants in MA,L, per epoch of construction, structural type and number of floors (data from Censos 2001).....	15
Table 3.4 – Number of dwellings per typological class and number of floor in MAL (data from Censos 2001)	16
Table 3.5 – Number of inhabitants per typological class and number of floors in MAL (data from Censos 2001).	17
Table 3.6 – Classes of ground type.	19
Table 6.1 – Number of deaths in each typological and soil classes; 475 years return period.	33
Table 6.2 – Lost area [10^6 m ²] per typological and soil classes; 475 years return period.....	34

1. INTRODUCTION

The project LESSLOSS – Risk Mitigation for Earthquakes and Landslides is a European integrated project developed within the framework of the Sixth Programme for Research, Technological Development and Demonstration of European Commission.

The project started in September, 2004, has a duration of 36 months, is coordinated by University of Pavia (Italy) and involves the participation of 46 European institutions.

Summarizing LESSLOSS objectives, it aims to promote a coordinated approach to the assessment of seismic risk, its environmental, urban and infrastructural impact, and prevention and protection strategies [Calvi & Pinho, 2004]. The LESSLOSS project addresses natural disasters, risk and impact assessment, natural hazard monitoring, mapping and management strategies, improved disaster preparedness and mitigation, development of advanced methods for risk assessment, methods of appraising environmental quality and relevant pre-normative research [Calvi & Pinho, 2004].

The LESSLOSS is a multidisciplinary project divided in eleven Research Components or Subprojects.

This report addresses the National Laboratory for Civil Engineering (LNEC) participation in Subproject 10 *Earthquake disaster scenario predictions and loss modelling for urban areas*. More precisely this report was developed in order to accomplish the 24 months LESSLOSS deliverable n° 85, which achieves loss estimates for the Metropolitan Area of Lisbon (MAL), for pre-defined scenarios earthquake. These loss estimations represent the reference situation to be compared with revised loss estimates after implementing mitigation actions with the ultimate goal of being established, in the next deliverable, the “most effective” mitigation strategy (deliverable 115).

The report is organized in 5 chapters. Besides this Introduction chapter 2 presents and justifies the revision of the reference ground motion earthquake scenarios.

Chapter 3 addresses loss estimations that will constitute the reference situation, in terms of physical damage, economic and human losses, before implementing mitigation actions. Curves of probabilistic seismic risk for the MAL region are also analyzed.

Chapter 4 analysis the major factors that contribute to loss estimations.

Final and general considerations are reported in Chapter 5.

2. REVISION OF REFERENCE GROUND MOTION EARTHQUAKE SCENARIOS

2.1. Justification

Since August 2005, when deliverable 83 concerning the *selection of 50 year and 500 year scenarios for Lisbon Metropolitan Area (MAL)* was accomplished, the work on seismic action scenarios selection and on the propagation of seismic motion suffered several progresses.

More specifically:

1. Seismic action scenarios were revised based on modal values derived from 3D disaggregation analyses in M and (X, Y) (magnitude and coordinates of bin source), instead of modal values derived from 2D disaggregation analysis in X and Y plus expected value of M , supported by Campos Costa *et al.* [2002]. Revised seismic hazard disaggregation analysis is presented in section 2.2. Details of its fundamentals and results were already published in Sousa [2006] and Sousa & Campos Costa [2006].
2. The seismological model used to assess offshore scenarios for MAL (explained in deliverable 83, UCAM, 2005) was recently calibrated.
3. The seismological model was updated in what concerns low frequencies range, with the introduction of the dynamic corner frequency [Motazedian & Atkinson, 2005].

Furthermore, in this report we would like to progress studying seismic risk for MAL region, before and after mitigation strategies, and consequently only two return periods (50 and 500 years) are not enough to perform this analysis.

Therefore this chapter presents the revised ground motion earthquake scenarios to be used on loss estimations. Upgrading and updating of models and data are detailed.

2.2. Seismic action scenarios based on hazard disaggregation

2.2.1. Seismic hazard disaggregation methodology

According to Montilla [2000], the first author to perform a seismic disaggregation process was Bernreuter [1992] intending to determine a controlling earthquake from a PSHA, that is, the earthquake that most significantly contributes, in terms of magnitude and distance to the hazard at a site, for a given level of ground motion.

Although this analysis is recent, it has been extensively discussed and applied, namely by Bazzurro [1998], Bazzurro and Cornell [1999], Campos Costa *et al.* [2002], Carvalho *et al.*

[2002], Chapman [1995], Cramer and Petersen [1996], Frankel *et al.* [1996], Frankel *et al.* [2000], Harmsen *et al.* [1999], McGuire [1995], Montilla [2000], Montilla and Cansado [2002], Sousa and Carvalho [2001] and Sousa *et al.* [2001]. Also some technical books [e.g. Kramer, 1996 and Pinto *et al.*, 2004] address the theme, even though briefly.

Seismic hazard disaggregation consists in the separation of the hazard exceedance contributions into different spaces of bins of the random variables of the process. The most used bin space is bi-dimensional (2D); that is, the relative contribution to the hazard is studied in terms of elementary bins of magnitude M , and earthquake to site distance, R or $\ln R$. McGuire [1995] included a third dimension into the procedure, analyzing the contribution to the hazard of 3D bins in M - R - ϵ . The variable ϵ , representing the third dimension, is a measure of the deviation of ground motion from the predicted (median) motion. Bazzurro and Cornell [1999] improved the disaggregation process evaluating hazard contributions in terms of M and ϵ and latitude and longitude, or Cartesian coordinates (X, Y) , instead of R .

Defining the procedure for seismic hazard disaggregation, Bazzurro and Cornell [1999], explain that a disaggregation process must initially evaluate the annual frequency of exceedance of a hazard level h , $\lambda_{H>h}$, in the region characterized by N_Z seismic source zones identified by the index k :

$$\lambda_{H>h} = \sum_{k=1}^{N_Z} v_k \cdot \int \int \int_{M R \epsilon} \mathcal{H}[H(M, R, \epsilon)_k - h] f_M(m)_k f_R(r)_k f_\epsilon(\epsilon)_k d\epsilon dr dm \quad (1)$$

where v_k is the mean annual rate of earthquake occurrence (with $M > m_{\min}$) in source zone k ; $\mathcal{H}[H(M, R, \epsilon)_k - h]$ is the Heaviside function that assumes the null value if $H(M, R, \epsilon)_k$ is less than h and the unit value otherwise; $f(\cdot)_k$ is the probability density function, in source zone k , of the considered random variables, admitted independent.

According to those authors the disaggregation of hazard can be achieved in two steps: (i) to accumulate in each bin its contribution to the global hazard and (ii) to divide the contribution accumulated in each bin by the total annual frequency of exceedance $\lambda_{H>h}$:

$$f_{M,R,\epsilon}(m, r, \epsilon | H > h) = \frac{\sum_k v_k \cdot \mathcal{H}[H(M, R, \epsilon)_k - h] f_M(m)_k f_R(r)_k f_\epsilon(\epsilon)_k}{\lambda_{H>h}} \quad (2)$$

Therefore, hazard disaggregation represents a conditional probability that, given the exceedance of a specified ground motion level, it has been caused by a certain combination of M and R and ϵ [McGuire, 1995]. In other words, when the contribution to hazard is accumulated in a 3D bin of M , R and ϵ the disaggregated hazard is represented by the joint probability mass function of M , R and ϵ , conditional on $H > h$ at the site [Bazzurro and Cornell, 1999].

Bazzurro and Cornell [1999] also emphasize that when the aim of a disaggregation procedure is to estimate the expected or the most likely event that cause the exceedance of the specified ground-motion level at the site, the results of hazard disaggregation are often summarized into central statistics, like means or modes. Discussion on whatever an earthquake scenario should be defined by a pair of mean values (\bar{M}, \bar{R}) or by modal values (\hat{M}, \hat{R}) resulting from hazard disaggregation, has taken place. Harmsen *et al.* [1999] decided to compute both mean and modal values pointing out that the use of (\hat{M}, \hat{R}) can be dependent on the dimension of the bins, whereas the use of (\bar{M}, \bar{R}) may correspond to earthquakes with negligible contribution to the hazard.

When probabilistic seismic hazard is disaggregated considering a 2D space of the random variables M and R , the bivariate conditional hazard distributions in M - R result from the integration of expression 2 regarding the deviate ε , conducting to a marginal bivariate distribution conditional on the exceedance of the hazard level at the site $H > h$:

$$f_{M,R}(m, r | H > h) = \int_{\varepsilon} f_{M,R,\varepsilon}(m, r, \varepsilon | H > h) d\varepsilon \quad (3)$$

In the next sections Portuguese probabilistic seismic hazard analysis is reviewed in order to perform its disaggregation.

Modal values of the above mentioned distribution (expression 3) substituting R by the pair (X, Y) are computed for each MAL parish, corresponding to the seismic scenarios that dominate each site hazard.

2.2.2. Revaluating seismic hazard for Mainland Portugal

Seismic hazard for Mainland Portugal is revaluated following Frankel [1995] methodology, considering that seismicity is not uniformly distributed inside source zones, but it is characterized by an empirical density function expressing the spatial distribution of events in the seismic catalogue (see figure 2.1). The remaining parameters characterizing seismic occurrence process in each source zone, like the Poissonian process and the exponential distribution of magnitudes, follows Sousa [1996] PSHA for the Portuguese region.

Macroseismic intensity I was chosen as the dependent variable in the attenuation models due to the scarcity of instrumental data in Portugal, mainly for high magnitudes. Five attenuation laws, developed by Sousa and Oliveira [1997] for that region, using macroseismic intensity (EMS) as dependent variable were applied.

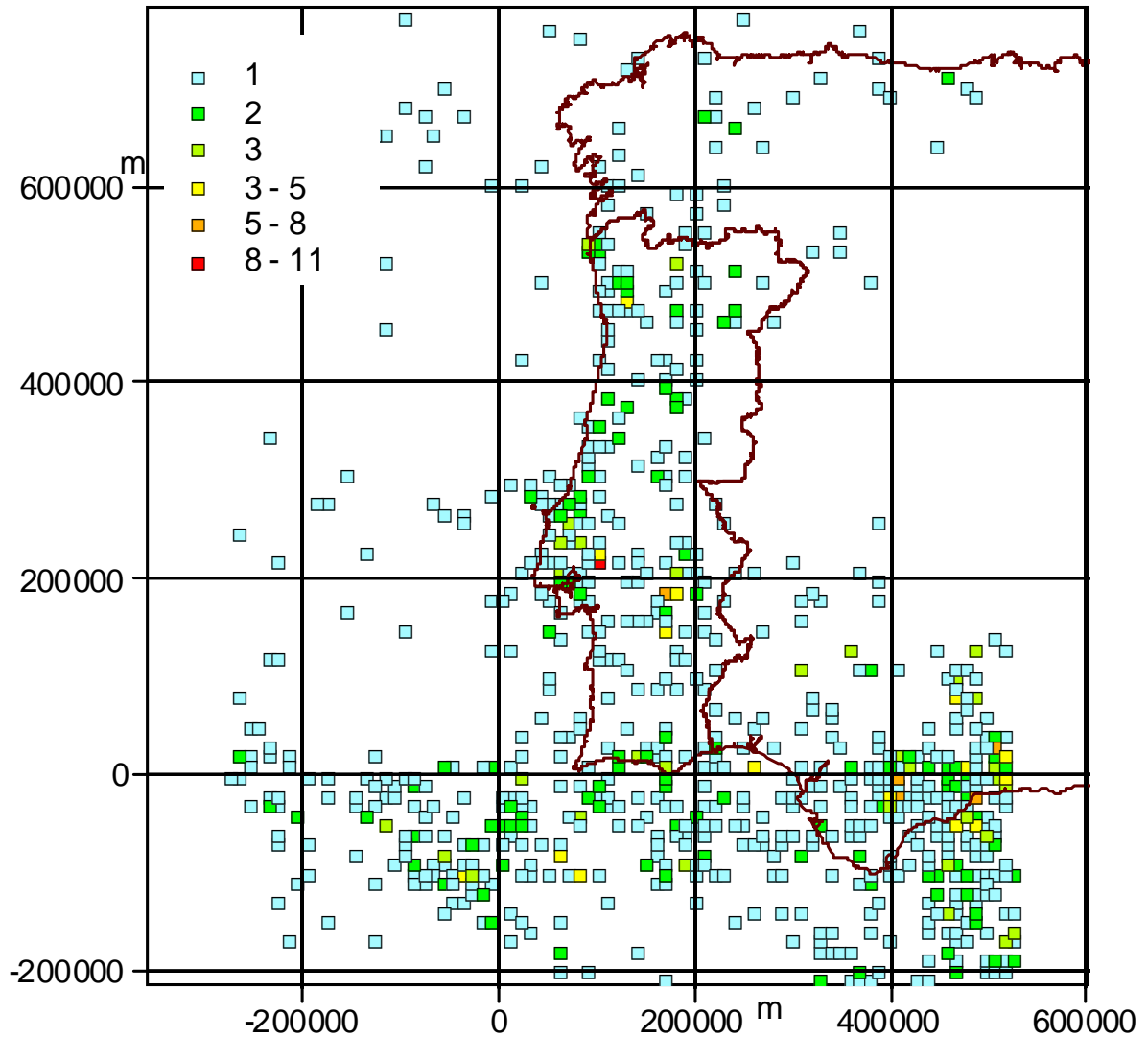


Figure 2.1 – Number of earthquakes with magnitude greater than 3.5 for each quadratic bin with 10×10 km; instrumental catalogue (year > 1909) without aftershocks [Sousa & Campos Costa, 2006].

Figure 2.2 exhibits the results of PSHA for Mainland Portugal. In this figure one identifies Lisbon site where disaggregation analysis will be graphically illustrated. Nevertheless, disaggregation analysis was carried out for the 277 parish of MAL, also zoomed in this figure.

In practice, the integrations in the PSHA (expression 1) were performed numerically and the elementary annual frequency of exceedance were assigned to the central point of each bin, with constant dimensions in the domain of analysis: $\Delta m = 0.1$ and $\Delta x = \Delta y = 10$ km, where Δx and Δy are elementary bins of Cartesian coordinates that allows the computation of distance bin ΔR .

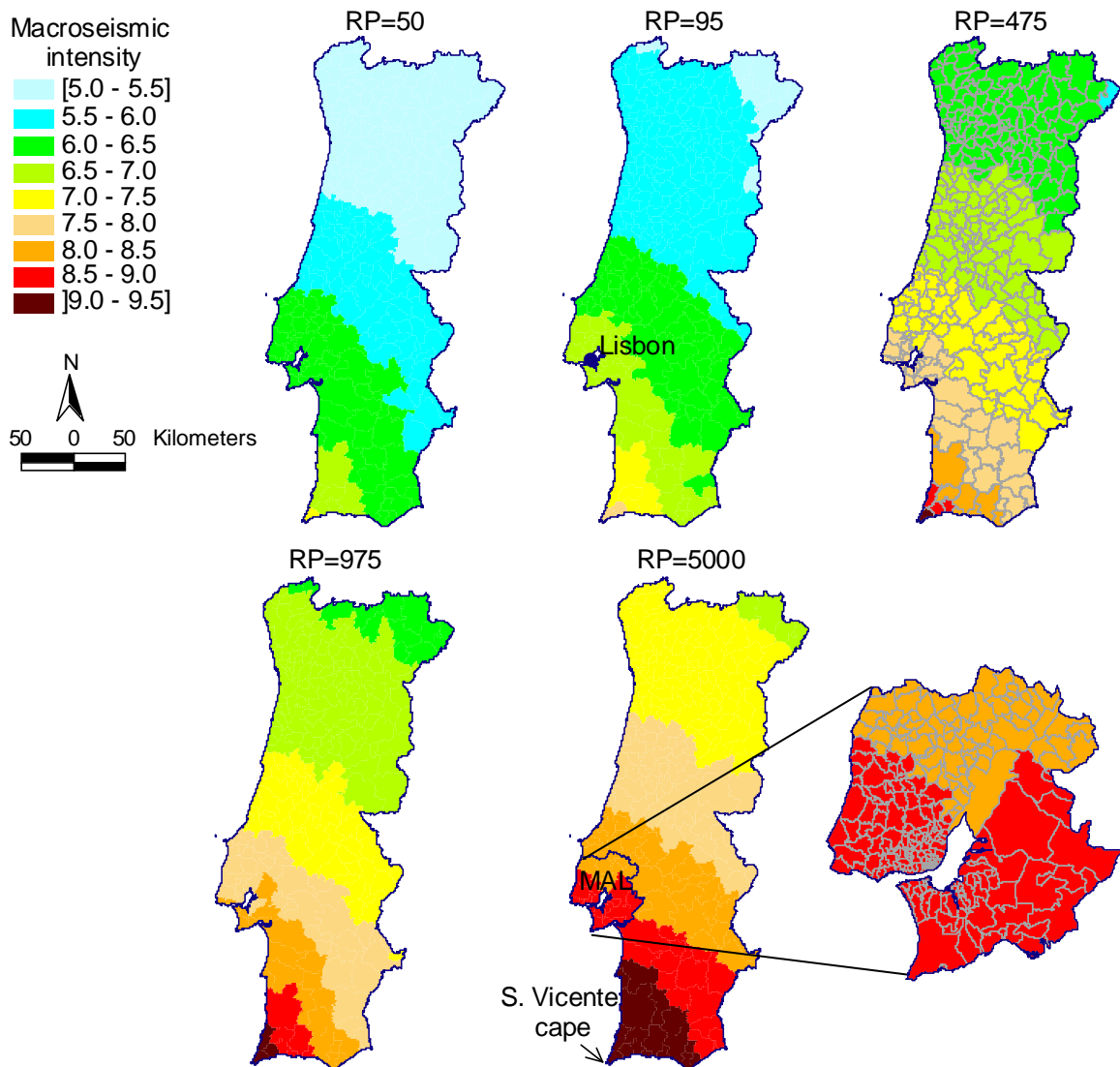


Figure 2.2 – Seismic hazard maps for Mainland Portugal for 50, 95, 475, 975 and 5000 return periods. 95 years RP: Lisbon site chosen for a more detailed graphic analysis of disaggregation. 475 years RP: 278 Portuguese counties. 5000 years RP: zoom of MAL region and its 277 parishes.

2.2.3. Disaggregation 3D in $M-(X, Y)$

Figure 2.3 illustrates the 3D seismic hazard disaggregation analysis for Lisbon site where random variables considered are simultaneously magnitude and source coordinates. To simplify the graphic representation the coordinates (X, Y) were substituted by source to site distance R .

The same figure exhibits modal values of the joint conditional distribution $f_{M,(X,Y)}(m, x, y | H > h)$, of random variables M and X, Y . In this figure total volume should be 1000‰, however, to lighten graphic representation contributions less than 0.01‰ were disregarded.

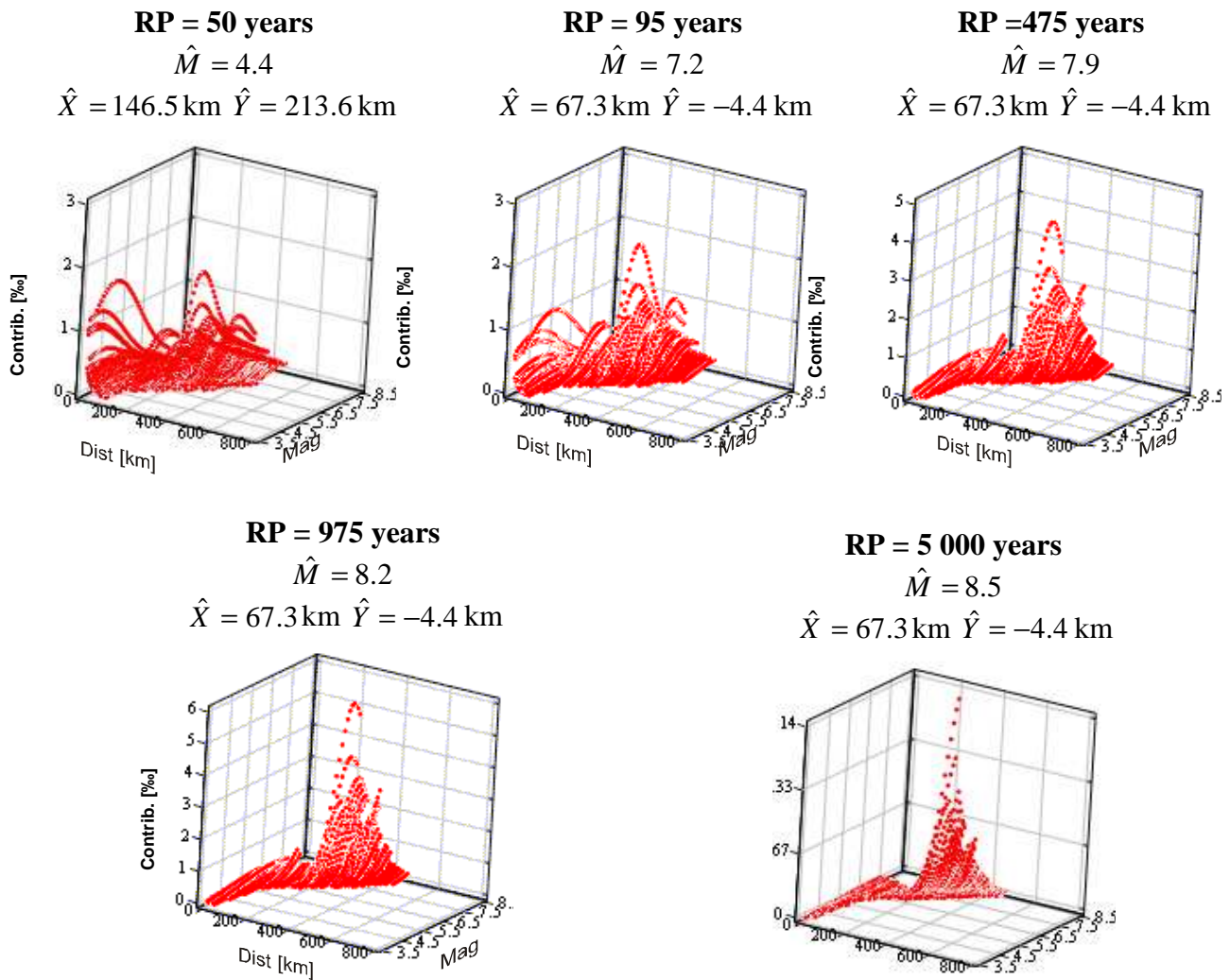


Figure 2.3 – Joint probability distribution or contribution of magnitude (Mag) and distance (X, Y) for 50, 95, 475, 975 and 5000 return periods for Lisbon site.

From the analysis of figure 2.3 for Lisbon site one may conclude that:

1. In what concerns 50 and 95 years return period, the joint conditional distribution shows a more accentuated multi-modal pattern than the remaining return periods, revealing the non uniqueness of dominant occurrence scenarios.
2. For the 50 years return period, disaggregation analysis indicates an important contribution of short distance modal scenario, although the second more important contribution corresponds to a long distance scenario, whereas for the remaining return periods disaggregation analysis specifies long distance modal scenarios.
3. For Lisbon site, all long distance scenarios, that is, modal scenarios for 95, 475, 975 and 5000 return periods are located in the same point only varying the scenario magnitude that increases with return period.

The disaggregation analysis for the great majority of MAL counties conducted to similar results. This conclusion leads to the adoption of Lisbon modal scenarios for the whole MAL. In fact, Lisbon County has the higher exposure of the region and seismic hazard doesn't vary considerably inside MAL (see figure 2.2), so one can expect that this County has the higher seismic risk of the region. Actually, Sousa [2006] concluded that Lisbon County contributed with 23% of the annualized earthquake economic loss of "MAL" region.

2.3. Finite fault propagation based on a seismological model

2.3.1. Calibrating seismological model

It was performed a new calibration of the seismological model, based on revised formulas for the quality factor, Q . The new relation, $Q=200f^{0.92}$ was derived from a revision of the work of Vales *et al.* [1998], considering the mean of all Q values obtained in several Portuguese stations using 97 records from the Lugo earthquake (Galiza, Spain) in 1997.

The calibration was performed using the dataset already presented in deliverable 83, which includes horizontal components of ground acceleration records obtained by the Portuguese digital accelerographic network, on hard sites. The changed parameters are the following:

Stress drop: For interplates scenario, it was adapted the values of 100 bars for the stress drop.

Anelastic Attenuation: The anelastic attenuation will be represented by the regional quality factor using the relation $Q=200f^{0.92}$.

Upper crust attenuation: A reasonable prediction of the strong motion recorded was found considering the upper crust attenuation with $f_{max} = 7\text{Hz}$ for interplates earthquakes.

Upper crust amplification factor: For interplates events the impedance function

$$F_{zi}(\omega) = \frac{2}{1 + \left(\frac{\omega_{zi}}{\omega}\right)^2} \quad \omega > \omega_{zi}, \text{ with } f_{zi}=0.25\text{Hz} \text{ represents a very good fit to data.}$$

Duration: The relationship $T = \frac{1}{f_0} + 0.02 \cdot R$ holds for interplates earthquakes.

All modeling parameters, including crustal and source properties, are presented in table 2.1

Table 2.1 – Seismological parameters.

Crustal thickness, D	25 km
Quality factor, $Q(f)$	$200f^{0.92}$
Geometric attenuation	$1/R$ ($R \leq 1.5D$) $1/R^0$ ($1.5D < R \leq 2.5D$) $1/R^{0.5}$ ($R > 2.5D$)
Distance-dependent duration	$0.02 R$
f_{max}	7 Hz
Shear-wave velocity, β	3.5 km/s
Crustal density, ρ	2.8 g/cm ³
Stress drop, $\Delta\sigma$	100 bar
Amplification function $F_{zi}(\omega)$	$f_{zi}=0.25\text{Hz}$

2.3.2. Upgrading seismological model

The modifications of the stochastic finite-fault method include the new concepts of “Dynamic corner frequency” and “Pulsing Subfaults” of Motazedian and Atkinson [2005].

In this approach, the corner frequency decreases with time as the rupture progresses in order to model the effects of finite-fault geometry on the frequency content radiated ground motions. At each instant the corner frequency depends on the cumulative ruptured area. The rupture begins with high corner frequencies and progress to lower corner frequencies.

The updated version also implements the concept of “Pulsing subfaults”, meaning that only a part of the rupture actively participate in the slip, at any time. This option does acknowledge the fact that the slip that occurs when a large rupture begins, may have stopped by the time that the rupture-propagation finally reaches the end of the fault.

Being so, the modified model has several significant advantages over the previous model, including conservation of radiated energy at high frequencies, regardless of subfault size and the ability to consider a percentage of the fault as actively pulsing at any time.

2.3.3. Attenuation laws derived from the seismological model

This calibrated and updated model was used as the basis for characterization of strong earthquakes for Portugal Mainland.

Response Spectra, for rock sites computed for many azimuths in Portugal mainland, for a set of offshore earthquakes covering a wide range of magnitudes (6.0 to 8.5 with increments of 0.5 units) and distances. The length and width of the fault plane are based on the moment magnitude relations of Wells & Coppersmith [1994] for reverse faults. In a first approximation the distance between site and hypocenter refers to the centre of the fault.

The simulated ground-motion amplitudes were fitted to a simple functional form, convenient to be used in seismic hazard analyses:

$$\log \text{PSA} = c1 + c2 M + c3 \log R + c4 R \quad (4)$$

where M is moment magnitude and R hypocentral distance.

Table 2.2 presents coefficients of ground motion relationships, for several periods.

Table 2.2 – Coefficients of the ground motion relations for rock sites

<i>Period [s]</i>	<i>c1</i>	<i>c2</i>	<i>c3</i>	<i>c4</i>
0.02	-0.5543	0.6099	-0.6439	-0.0021
0.05	-0.5013	0.6089	-0.6489	-0.0021
0.1	-0.2205	0.6036	-0.6321	-0.0022
0.2	-0.1324	0.6032	-0.5999	-0.0021
0.4	-0.3544	0.6120	-0.6214	-0.0020
1.0	-1.4621	0.6705	-0.4878	-0.0020
1.5	-1.8987	0.7192	-0.5568	-0.0018
2.0	-2.4512	0.7754	-0.5956	-0.0017
2.5	-2.7590	0.8111	-0.6472	-0.0017
3.0	-3.0264	0.8440	-0.7137	-0.0016
5.0	-3.3982	0.9148	-0.9927	-0.0013
PGA	-0.7726	0.6216	-0.6028	-0.0021
PGV	-2.4469	0.6947	-0.6440	-0.0018

It is worth mentioning that, even though regression was made considering hypocentral distance, the amplitude of the ground motion reflects the finite fault behavior and it is, of course, controlled by the rupture length of the fault, the closest distance to the fault and directivity effects. Equations are justified by the full theory behind the stochastic model, presented in deliverable 83.

2.4. Ground motion maps

Ground motion maps (PGA) for 50 years and 475 years return periods are shown in figures 2.4 and 2.5. The magnitude and distance of those scenarios are specified in figure 2.3.

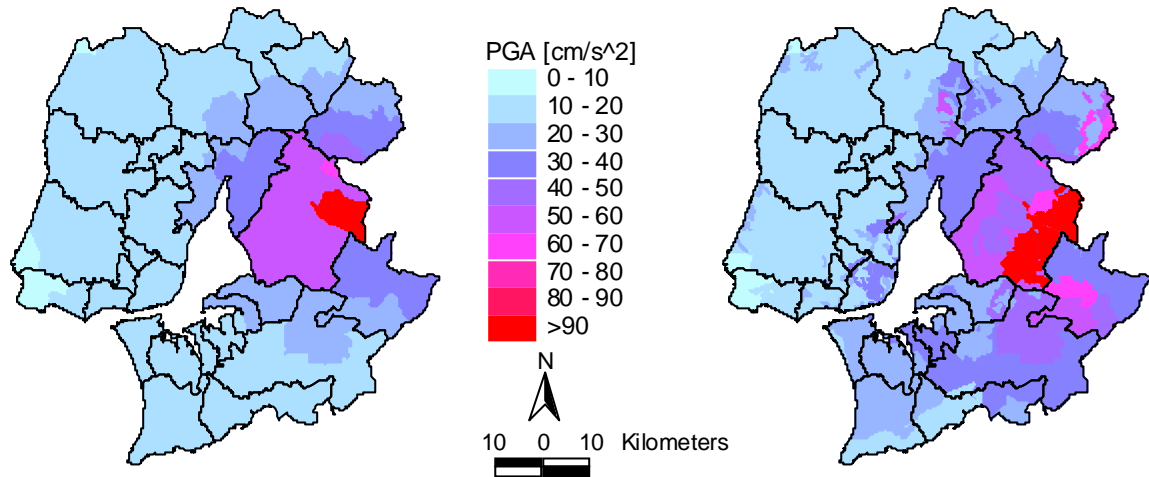


Figure 2.4 – Peak ground acceleration for bedrock (left) and considering soil columns (right) for MAL, for the 50 years return period.

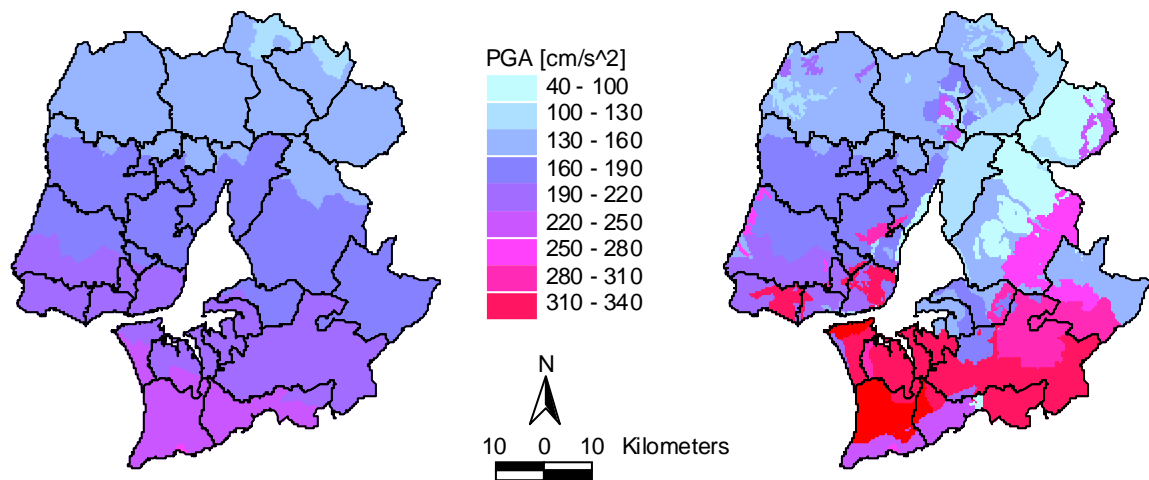


Figure 2.5 – Peak ground acceleration for bedrock (left) and considering soil columns (right) for MAL, for the 475 years return period.

Ground motion maps for the 475 years return period present higher values for PGA in comparison with ground maps presented in deliverable 83 due to the new calibration of the seismological model and to the change of the scenario magnitude as a result of a 3D PSHA disaggregation (M=7.9 instead of M=7.6).

Analyzing figure 2.5 it is clear that PGA soil amplification is particularly pronounced in the South margin of Tagus River.

3. REFERENCE LOSS ESTIMATIONS

3.1. Exposure analysis

3.1.1. Typological classification

The typological classification for MAL building stock was already presented in deliverable 81. Following the criteria used to classify the vulnerability of MAL housing stock, it was possible to identify 7 typological classes according to the building construction epoch and to their structural type (table 3.1 left).

Each typological class includes 7 typologies according to the classes of number of floors (table 3.1 right).

The aggregation of 325 original typologies (9 epochs of construction \times 5 structural types \times 7 classes for the number of floors) is justified in order to emphasise the correlation of losses estimates and building typological classes.

Table 3.1 – Typological and floor classes.

<i>Typological classes</i>	<i>No of floors</i>
Adobe + rubble stone + others	1
Masonry before 1960	2
Masonry 1961-85	3
Masonry 1986-01	4
RC before 1960	5 a 7
RC 1961-85	8 a 15
RC 1986-01	+ de 15

In deliverable 81 the exposure was presented in terms of number of buildings, because one intended to carry out the characterization of seismic vulnerability of MAL. As the present report focuses on seismic risk analysis the exposure is now characterized in terms of dwellings and people at risk.

The analysis of Portuguese Censos 2001 [INE, 2002] conducted to the classification of MAL dwellings (table 3.2) and inhabitants (table 3.3) per epoch of construction, structural type and number of floors.

Table 3.2 – Number of familiar dwellings in MAL, per epoch of construction, structural type and number of floors (Censos 2001).

Epoch	No. of floors	RC	Masonry with RC floors	Masonry without RC floors	Adoberubble stone	Others (wood, steel, etc.)
Before 1919	1	0	0	8 724	7 548	158
	2	0	0	7 188	4 277	97
	3	0	0	6 544	2 035	52
	4	0	127	8 948	0	95
	5 a 7	0	42	6 303	0	95
	8 a 15	0	0	0	0	0
	+ de 15	0	0	0	0	0
Total		0	169	37707	13860	497
1919 to 1945	1	3547	6434	11590	5406	132
	2	2273	4417	6382	1463	33
	3	3221	3575	6222	526	47
	4	3177	4446	6902	0	57
	5 a 7	3945	10839	5185	0	24
	8 a 15	1998	0	0	0	8
	+ de 15	0	0	0	0	0
Total		18161	29711	36281	7395	301
1946 to 1960	1	8548	11354	10678	3020	138
	2	8488	8887	3740	679	33
	3	11290	6755	2272	398	27
	4	19877	9145	3090	0	16
	5 a 7	21120	12098	1575	0	30
	8 a 15	10739	0	0	0	0
	+ de 15	0	0	0	0	0
Total		80062	48239	21355	4097	244
1961 to 1970	1	15363	16912	6616	1047	212
	2	15514	10423	1433	292	19
	3	17048	5920	923	120	10
	4	41079	7975	1126	0	13
	5 a 7	49919	10394	579	0	21
	8 a 15	35320	0	0	0	0
	+ de 15	2119	0	0	0	0
Total		176362	51624	10677	1459	275
1971 a 1980	1	20453	19695	3928	576	368
	2	23362	14534	955	178	29
	3	16340	6132	410	110	1
	4	42114	7413	631	0	24
	5 a 7	66037	8999	425	0	20
	8 a 15	65822	0	0	0	0
	+ de 15	4397	0	0	0	28
Total		238525	56773	6349	864	470
1981 to 1985	1	11039	9652	1745	285	268
	2	15285	8195	362	105	37
	3	7775	2641	166	34	18
	4	13071	2548	183	0	52
	5 a 7	28148	3675	163	0	29
	8 a 15	29648	0	0	0	148
	+ de 15	3789	0	0	0	0
Total		108755	26711	2619	424	552
1986 to 1990	1	8484	6483	932	187	131
	2	11619	6387	245	108	24
	3	7423	2249	128	18	7
	4	12928	2151	113	0	0
	5 a 7	29734	3630	144	0	0
	8 a 15	28408	0	0	0	15
	+ de 15	2874	0	0	0	0
Total		101470	20900	1562	313	177
1991 to 1995	1	6769	5645	659	218	148
	2	9563	5053	288	86	27
	3	7247	2210	190	36	10
	4	11854	1942	175	0	16
	5 a 7	31267	4747	142	0	24
	8 a 15	34915	0	0	0	0
	+ de 15	2154	0	0	0	0
Total		103769	19597	1454	340	225
1996 to 2001	1	7027	5394	622	225	110
	2	13295	7597	300	173	28
	3	10712	2998	294	69	21
	4	16218	3279	295	0	22
	5 a 7	43038	3900	248	0	31
	8 a 15	39980	0	0	0	18
	+ de 15	3017	0	0	0	0
Total		133287	23168	1759	467	230
Total	Tip. Struct.	235256	149764	66111	24072	1967
1 floor	2 floors	3 floors	4 floors	5 a 7 floors	8 a 15 floors	+ de 15 floors
228470	193473	134224	221102	346570	247019	18378

Table 3.3 – Number of inhabitants in MA,L, per epoch of construction, structural type and number of floors (data from Censos 2001).

Epoch	No. of floors	RC	Masonry with RC floors	Masonry without RC floors	Adobe rubble stone	Others (wood, steel, etc.)
Before 1919	1	0	0	13 281	10 344	199
	2	0	0	13 206	6 681	164
	3	0	0	10 347	3 414	99
	4	0	184	14 331	0	257
	5 a 7	0	75	10 183	0	156
	8 a 15	0	0	0	0	0
	+ de 15	0	0	0	0	0
	Total	0	259	61348	20439	875
1919 a 1945	1	5831	11136	17392	7544	224
	2	4041	8124	10275	2287	56
	3	5356	6245	9838	924	87
	4	5644	7649	11424	0	108
	5 a 7	6641	19003	8940	0	42
	8 a 15	3499	0	0	0	19
	+ de 15	0	0	0	0	0
	Total	31012	52157	57869	10755	536
1946 a 1960	1	16461	21555	17427	4730	197
	2	17024	17619	6876	1177	57
	3	21555	13653	3970	612	56
	4	36956	16828	5308	0	38
	5 a 7	38228	22267	2886	0	56
	8 a 15	18896	0	0	0	0
	+ de 15	0	0	0	0	0
	Total	149120	91922	36467	6519	404
1961 a 1970	1	30262	33823	11265	1666	522
	2	32936	22694	2620	561	51
	3	35775	12041	1776	220	27
	4	84939	16094	2196	0	35
	5 a 7	101269	20043	1103	0	40
	8 a 15	69278	0	0	0	0
	+ de 15	4421	0	0	0	0
	Total	358880	104695	18960	2447	675
1971 a 1980	1	45115	44635	7842	1116	967
	2	56019	35515	2262	376	43
	3	37177	14369	784	238	0
	4	94638	16880	1352	0	65
	5 a 7	147302	19124	1042	0	34
	8 a 15	140714	0	0	0	0
	+ de 15	8811	0	0	0	44
	Total	529776	130523	13282	1730	1153
1981 a 1985	1	22890	19498	4227	551	605
	2	36089	19012	769	202	60
	3	18511	6399	278	77	28
	4	30056	5944	350	0	107
	5 a 7	62683	7681	505	0	49
	8 a 15	66407	0	0	0	348
	+ de 15	7681	0	0	0	0
	Total	244317	58534	6129	830	1197
1986 a 1990	1	17514	13409	2008	378	78
	2	25972	15278	419	225	18
	3	17104	5226	217	44	1
	4	28633	4880	200	0	0
	5 a 7	66138	8907	293	0	0
	8 a 15	64247	0	0	0	34
	+ de 15	6198	0	0	0	0
	Total	225806	47700	3137	647	131
1991 a 1995	1	13326	11247	1166	356	135
	2	22237	12621	522	196	5
	3	17059	5099	363	74	23
	4	26661	3944	350	0	27
	5 a 7	69034	10283	231	0	57
	8 a 15	79735	0	0	0	0
	+ de 15	5122	0	0	0	0
	Total	233174	43194	2632	626	247
1996 a 2001	1	13244	10883	1002	373	82
	2	28675	16003	523	322	33
	3	20803	5733	410	102	30
	4	27447	5543	446	0	37
	5 a 7	74417	6693	331	0	52
	8 a 15	72627	0	0	0	33
	+ de 15	5119	0	0	0	0
	Total	242332	44855	2712	797	267
Total	Tip. Struct.	235256	149764	66111	24072	1967
1 floor	2 floors	3 floors	4 floors	5 a 7 floors	8 a 15 floors	+ de 15 floors
211660	142052	45451	31941	33852	11712	502

Figure 3.1 shows the percentage of dwellings in MAL per typological classes and table 3.4 the distribution of each typological class per number of floors. Similar information is presented in figure 3.2 and table 3.5 referring to MAL inhabitants. The average number of inhabitants per dwelling, in MAL, is 2.1.

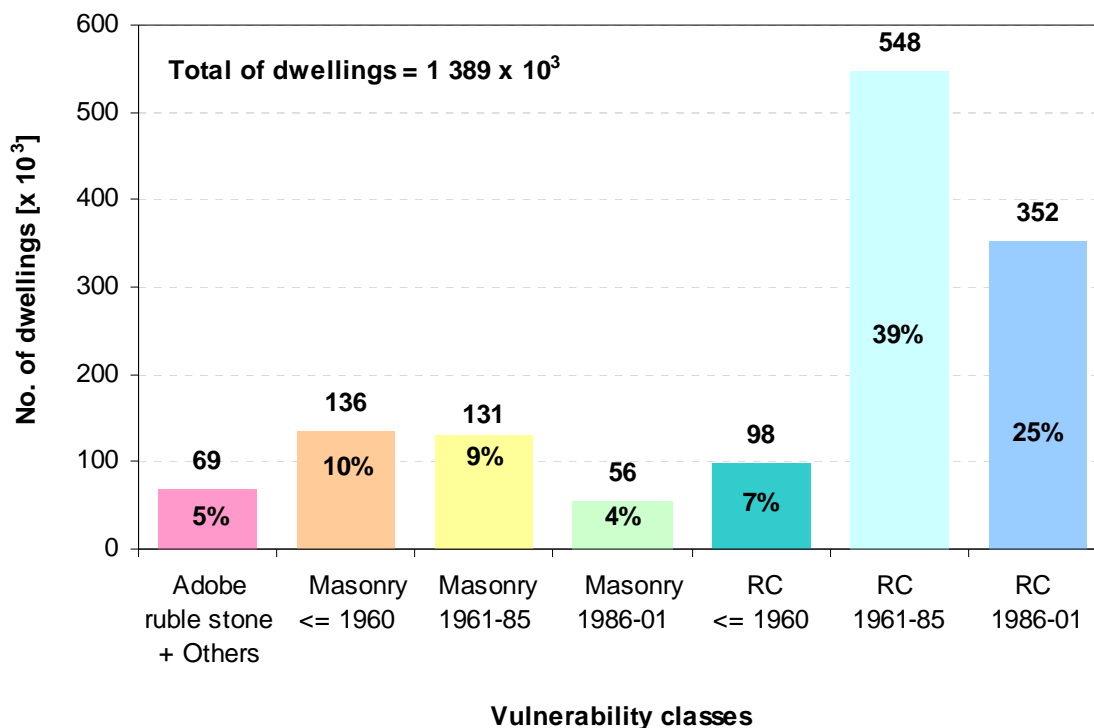


Figure 3.1 – Distribution of dwellings per typological classes in MAL (data from Censos 2001).

Table 3.4 – Number of dwellings per typological class and number of floor in MAL (data from Censos 2001)

Type./ No.floors	Adobe + rubble stone+Others	Masonry ≤ 1960	Masonry 1961-85	Masonry 1986-01	RC ≤ 1960	RC 1961-85	RC 1986-01
1	28 901	40 056	58 548	19 735	12 095	46 855	22 280
2	14 876	23 426	35 902	19 870	10 761	54 161	34 477
3	10 083	18 824	16 192	8 069	14 511	41 163	25 382
4	9 116	23 710	19 876	7 955	23 054	96 264	41 127
5-7	6 452	29 739	0	0	25 065	168 339	116 975
7-15	0	0	0	0	12 737	130 790	103 492
+15	0	0	0	0	0	10 305	8 073
Total	69 428	135 755	130 518	55 629	98 223	547 877	351 806

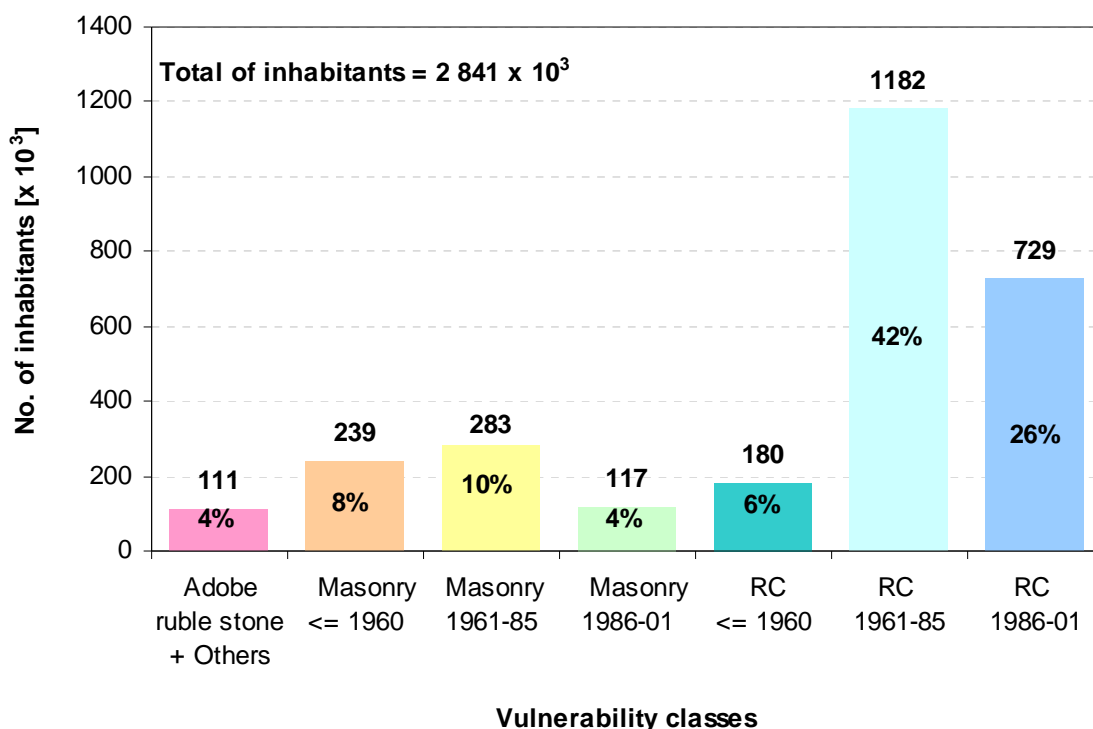


Figure 3.2 – Distribution of inhabitants per typological classes in MAL (data from Censos 2001).

Table 3.5 – Number of inhabitants per typological class and number of floors in MAL (data from Censos 2001).

Type./ No.floors	Adobe + rubble stone + Others	Masonry ≤ 1960	Masonry 1961-85	Masonry 1986-01	RC ≤ 1960	RC 1961-85	RC 1986-01
1	43 348	67 510	121 290	39 715	22 292	98 267	44 084
2	25 720	42 894	82 872	45 366	21 065	125 044	76 884
3	16 403	33 706	35 647	17 048	26 911	91 463	54 966
4	14 734	41 393	42 816	15 363	42 600	209 633	83 012
5-7	10 437	53 171	0	0	44 869	360 752	236 559
7-15	0	0	0	0	22 395	276 399	217 043
+15	0	0	0	0	0	20 913	16 483
Total	110 642	238 674	282 625	117 492	180 132	1 182 471	729 031

3.1.2. Soil classification

The influence of soil condition on damage must also be analysed in order to study the most effective mitigation strategy, in what concerns building vulnerability reducing.

LNECloss algorithms (see deliverable 81) take into account site effects due to soil dynamic amplification by means of an equivalent stochastic nonlinear one-dimensional ground response analysis of stratified soil profile units designed for the region.

For MAL region there were identified 37 soil columns units as shown in figure 3.3 [Carvalho *et al.*, 2002].

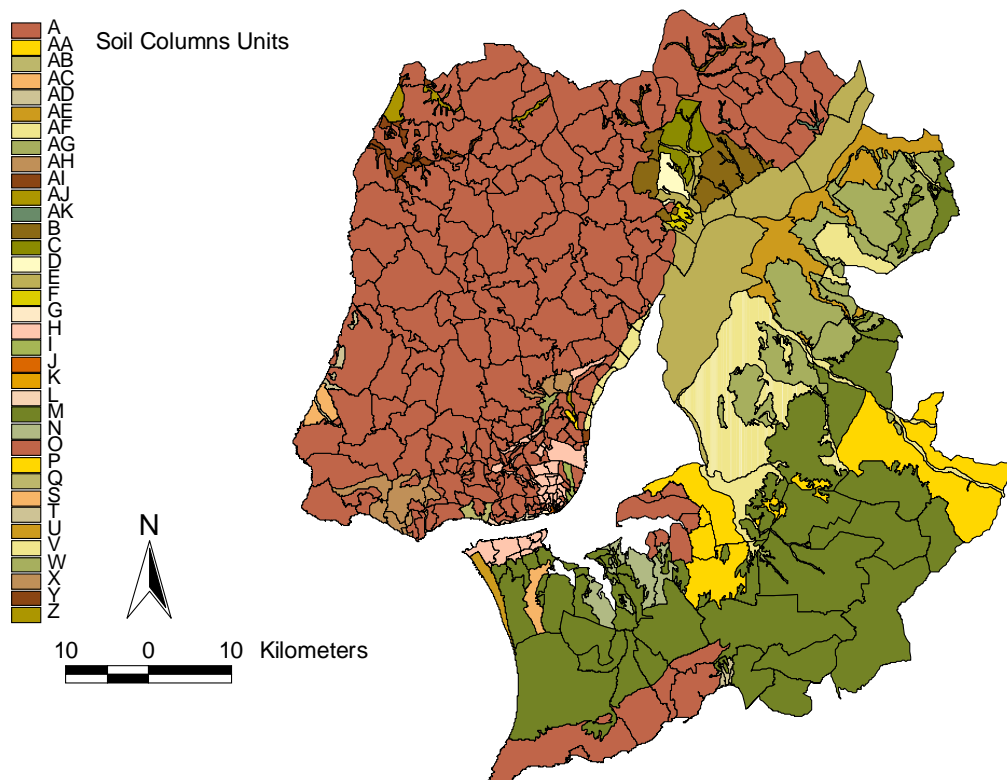


Figure 3.3 – Soil columns units for MAL [Carvalho *et al.*, 2002].

Following a similar criterion used for building classification (section 3.1.1) and although LNECloss works with the 37 soil column units presented above, a classification that aggregates results (table 3.6, figure 3.4) was used in order to emphasise the correlation of losses estimates and soil classification. For that purpose three broader soil classes were created (Rock and Hard, Intermediate and Soft) according to classes of shear wave velocity v_s values adapted from Portuguese National Annexes of Eurocode 8 [IPQ, 2000].

The method applied to lump the 37 soils column units was the following:

1. Taking into account the transfer function derived from the 50 years return period (very low seismic input) the lowest natural frequency f_1 of each soil column unit was obtained. Additionally for each soil unit the bedrock depth H (identified when $v_s > 600 \text{ m/s}$) was also taken into account.
2. An equivalent apparent shear wave velocity v_s was subsequently obtained from those two values (f_1 and H) following the well known expression of the *characteristic site period* [Kramer, 1996]:

$$v_s = f_1 \cdot 4H \quad [\text{m/s}] \quad (5)$$

Table 3.6 – Classes of ground type.

Ground type	Stratigraphic profile	v_s [m/s]
A	Rock and hard soil	> 350
B	Intermediate soil	200-350
C	Soft soil	< 200

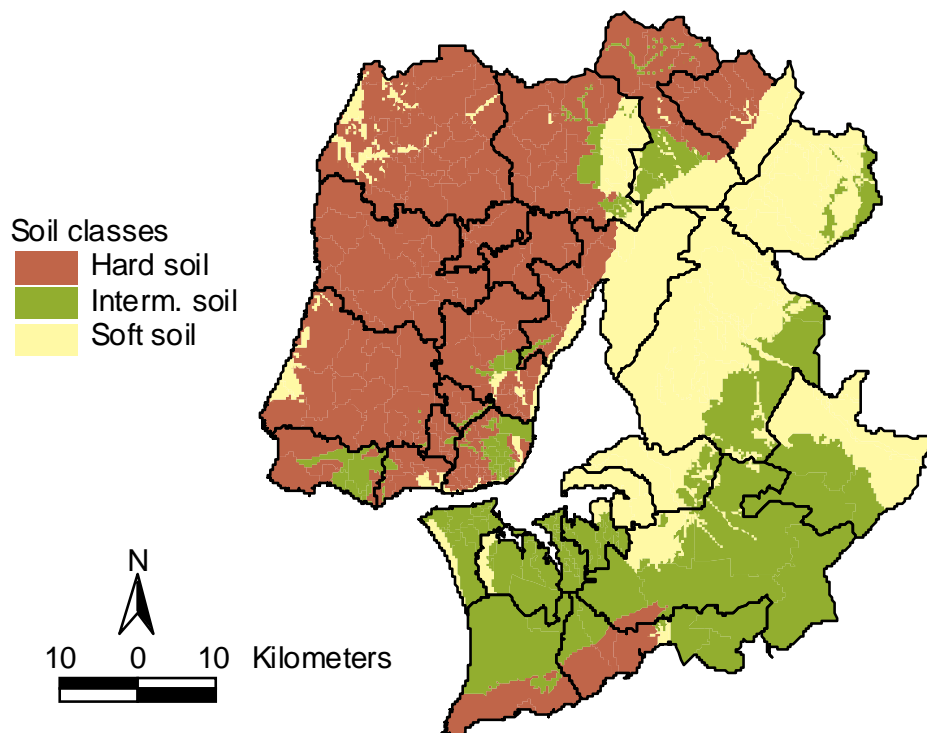


Figure 3.4 – Geographic distribution of ground type for MAL, according to Portuguese version of EC8.

3.1.3. Exposure analysis by typological and soil classification

Figures 3.5 to 3.7 put crosswise the number of familiar dwellings, inhabitants and total building areas [m²] per typological class and ground type, respectively.

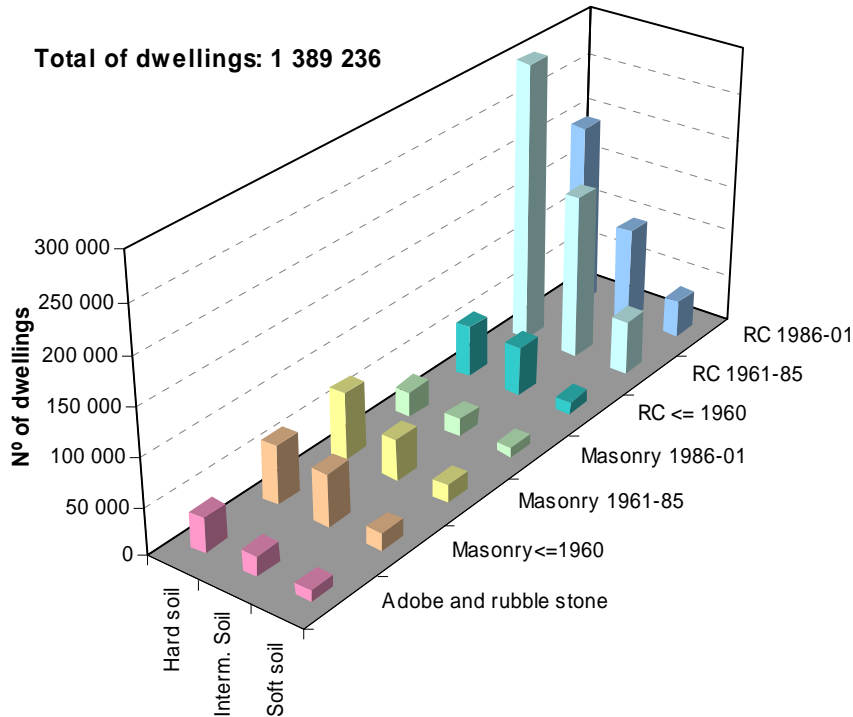


Figure 3.5 – Number of dwellings per typological class and ground type.

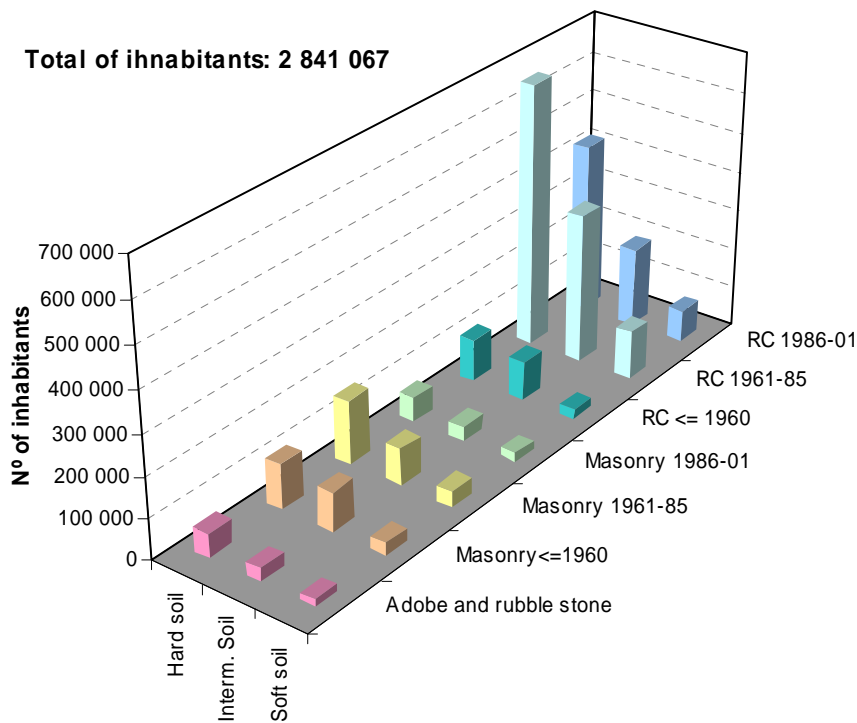


Figure 3.6 – Number of inhabitants per typological class and ground type.

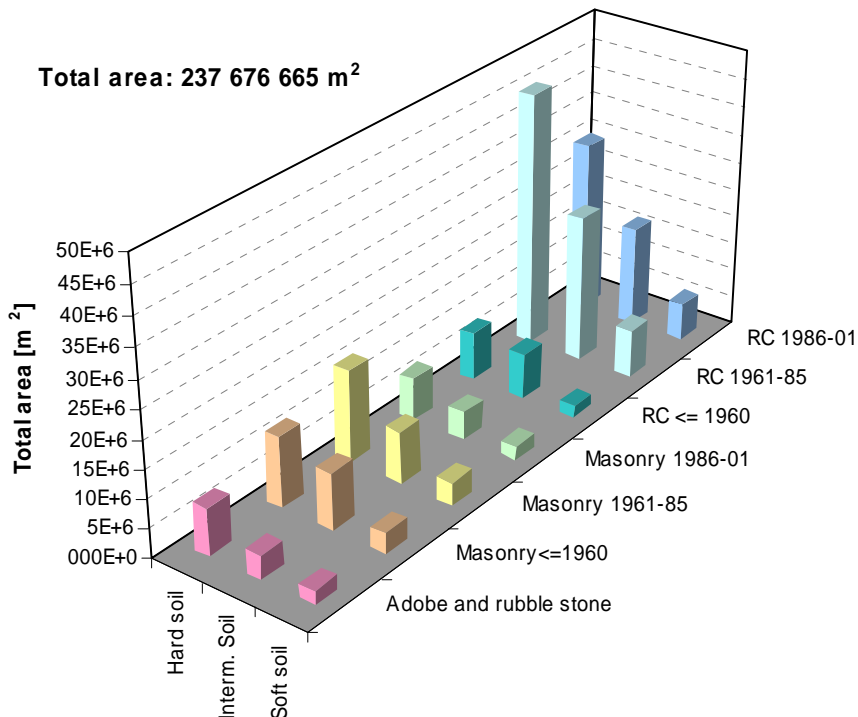


Figure 3.7 – Total area [m²] in MAL per typological class and ground type.

3.2. Physical damage

Figure 3.8 illustrates the maps of loss estimations for the reference situation before implementing mitigation actions, in terms of Severely and Completely Damaged¹ dwellings in MAL. Damages were computed for 50 and 475 years return period scenarios. Severely and Completely Damaged dwellings, for the 50 years return period, were estimated as 0% for all MAL parishes, therefore the correspondent maps weren't plotted.

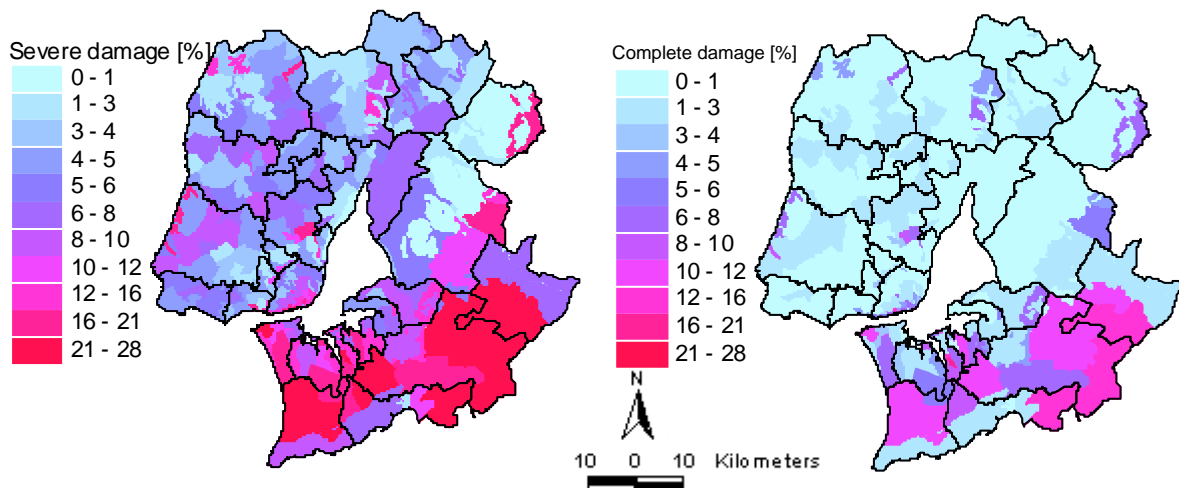


Figure 3.8 – Reference situation: maps of severely and completely damaged dwellings. Losses for 475 return periods scenarios.

¹ See deliverable 81 for definition of damage states.

3.3. Human losses

Figure 3.9 presents the maps of human losses, for the reference situation, before implementing mitigation actions. Human losses were computed for 50 and 475 years return periods. As a consequence of 0% of Severely and Completely damaged dwellings, there are no casualties for the lower return period. Being so, map for 50 years return period is not presented.

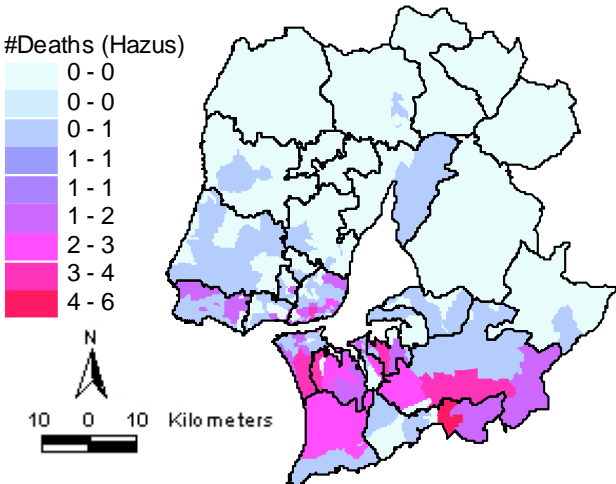


Figure 3.9 – Reference situation: maps of human losses for 475 return period scenario.

3.4. Economic losses

Figure 3.10 shows the maps of economic losses in terms of equivalent lost area, for the reference situation, before implementing mitigation actions. Losses were computed for the 475 years return period scenario taking into account FEMA & NIBS [1999] economic model.

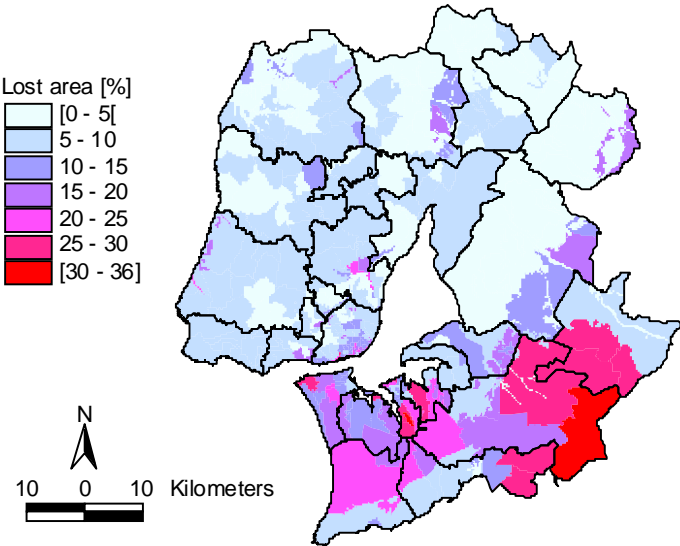


Figure 3.10 – Reference situation maps of economic losses for 475 return period scenario.

4. ANALYSIS OF REFERENCE SCENARIOS

Figures 4.1 to 4.8 were designed in order to investigate which are the combinations of typological and soil classes responsible for higher losses in MAL.

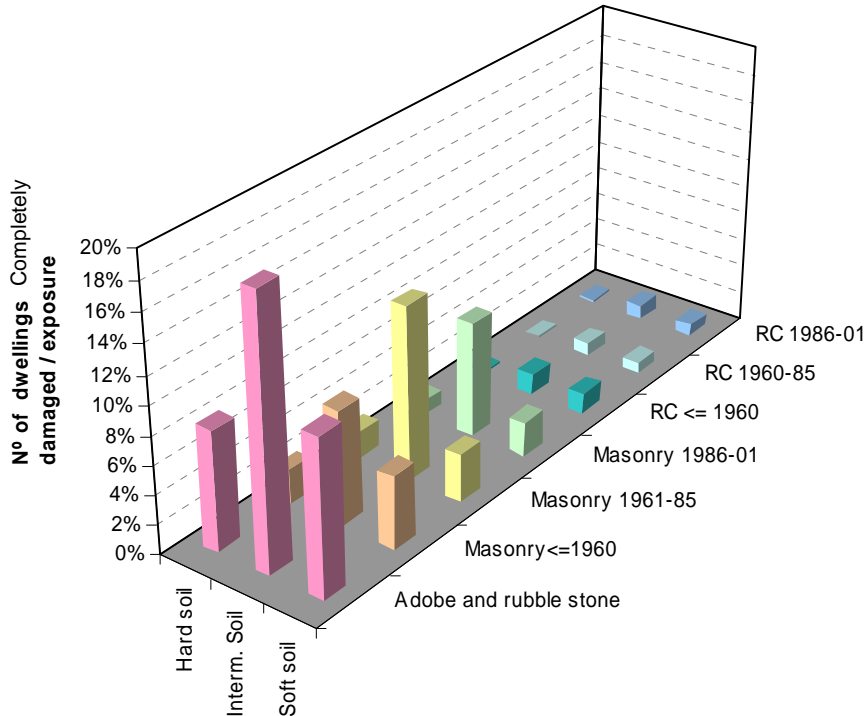


Figure 4.1 – Number of Completely Damaged dwellings normalized by exposure in each typological and soil classes; 475 years return period.

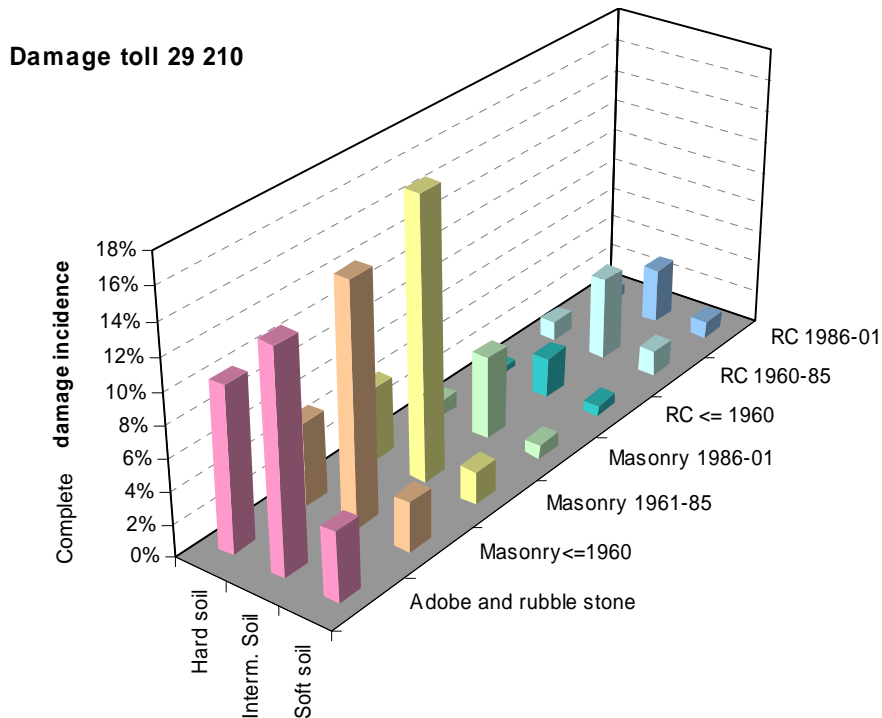


Figure 4.2 – Number of Completely Damaged dwellings in each typological and soil classes normalized by Completely Damaged dwellings toll; 475 years return period.

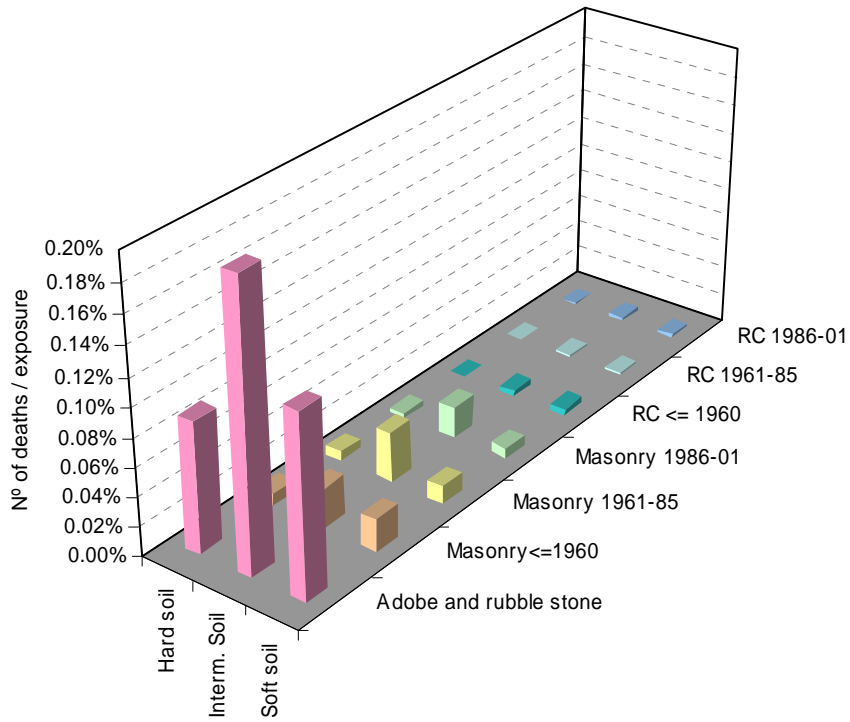


Figure 4.3 – Number of deaths normalized by exposure in each typological and soil classes; 475 years return period.

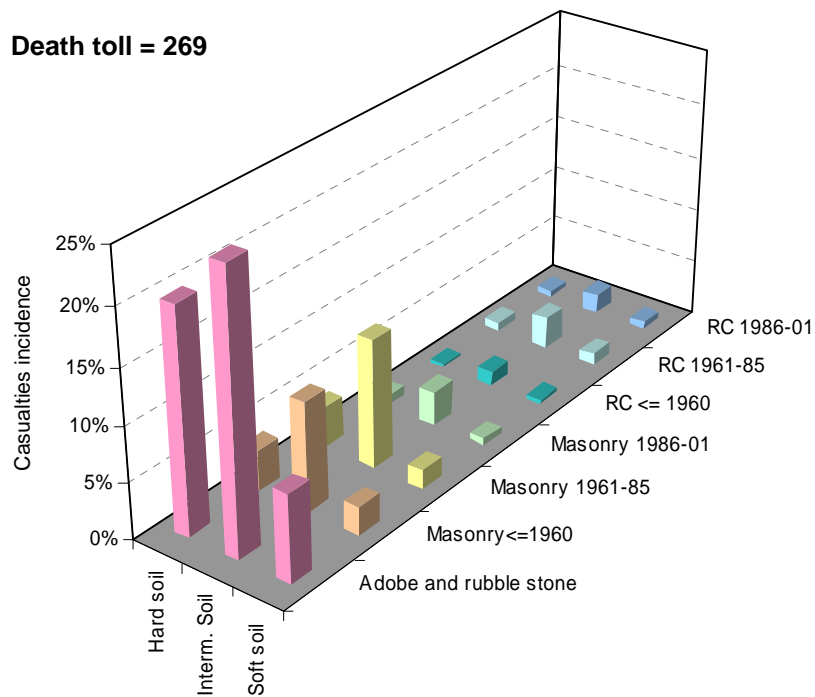


Figure 4.4 - Number of deaths in each typological and soil classes normalized by death toll; 475 years return period.

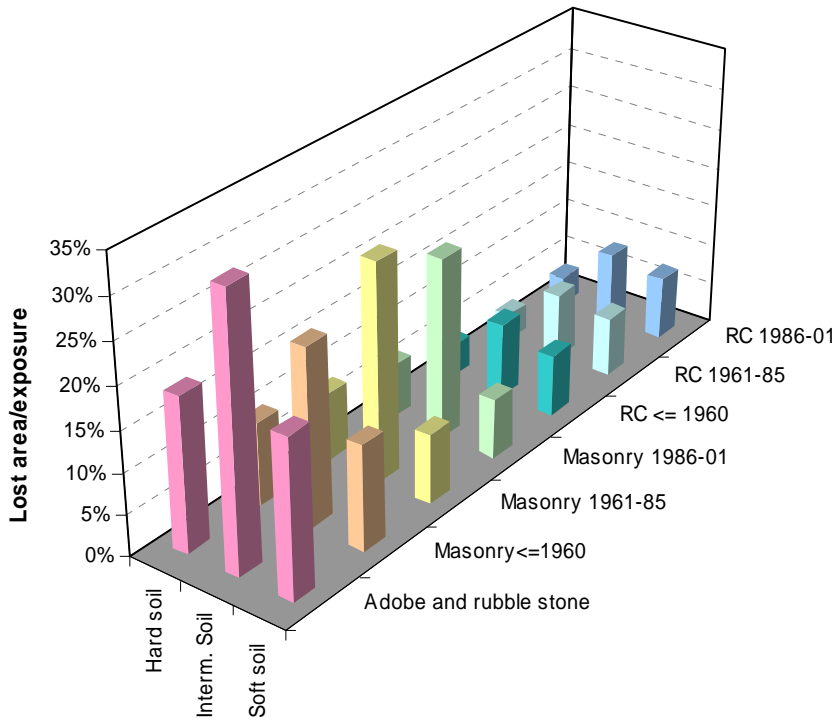


Figure 4.5 – Lost area normalized by exposure in each typological and soil classes; 475 years return period.

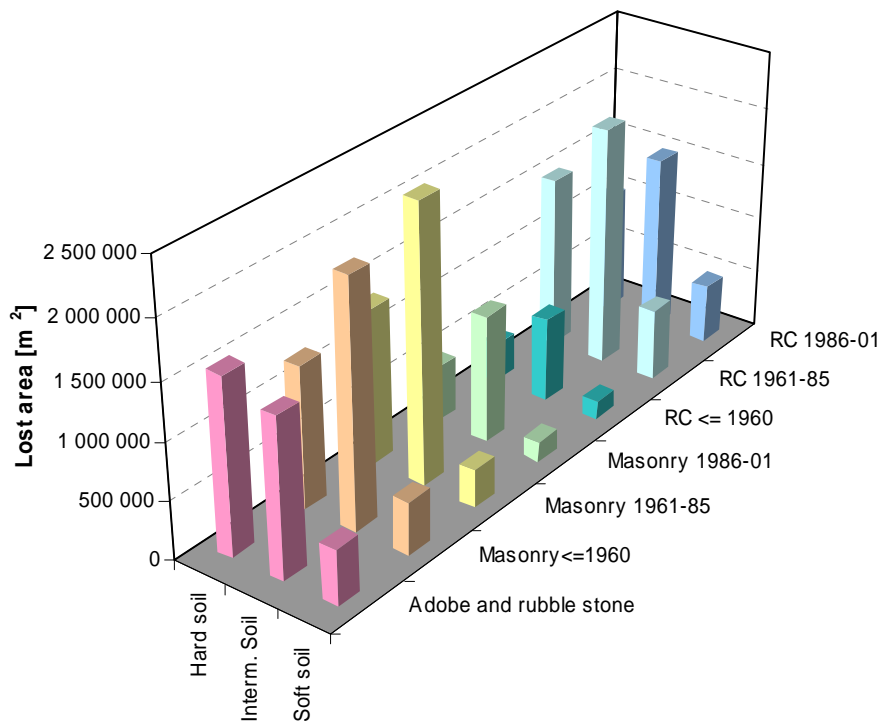


Figure 4.6 - Lost area per typological and soil classes; 475 years return period.

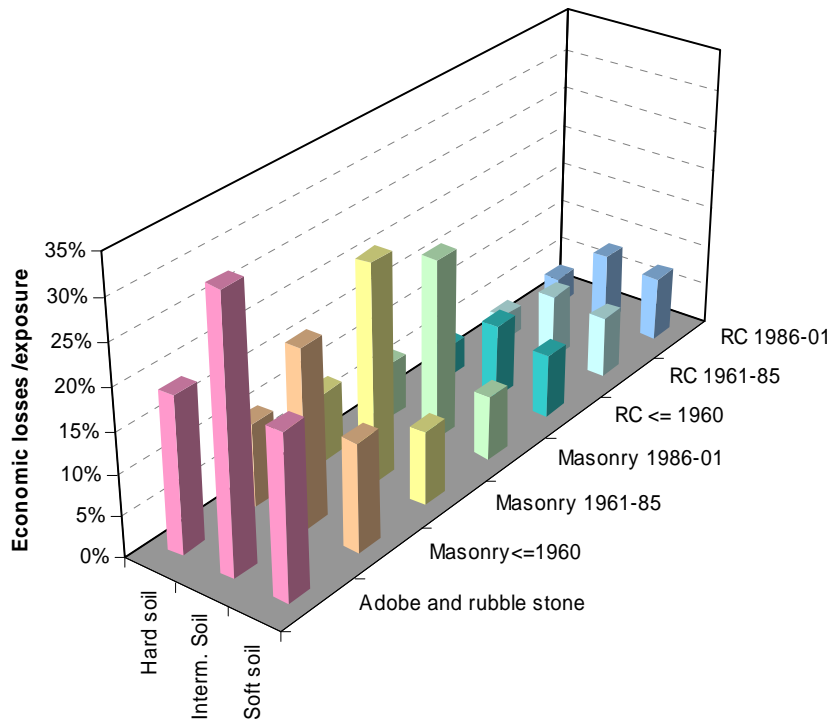


Figure 4.7 – Economic losses normalized by exposure in each typological and soil classes; 475 years return period.

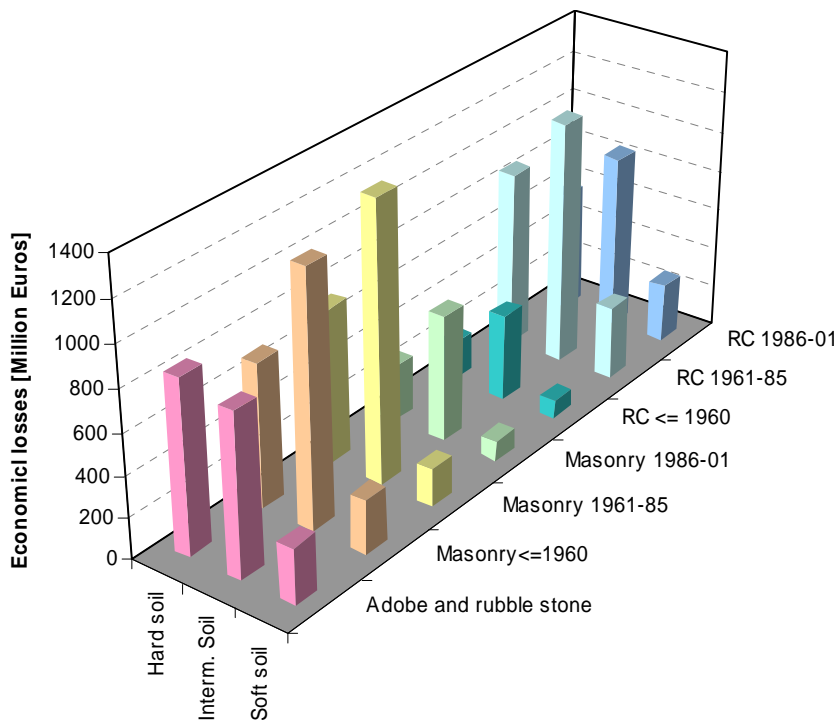


Figure 4.8 - Economic losses per typological and soil classes; 475 years return period.

The analysis of reference situation, for the 475 return period, includes three different kinds of loss indicators, related to physical damage, human losses and economic losses:

4.1. Physical damage

The analysis of physical damage, in relative terms (that is, normalized by the exposure in each typological and soil classes) shows that the elements with higher contribution to damage are typological classes *Adobe and rubble stone* and *Masonry 1961-85* located in *intermediate soils* (figure 4.1). This reflects the higher vulnerability and fragility of the above mentioned typological classes.

The dwellings in typological class *Masonry 1961-85* built in *intermediate soil* show the highest contribution to the toll of Completely Damaged dwellings (figure 4.2). *Masonry before 1960* in *intermediate soil* and *Adobe and rubble stone* in *hard* and *intermediate soil* classes also contribute significantly to that toll (figure 4.2). Among *RC* typological classes the one belonging to *1961-85* epoch, located in *intermediate soils*, presents the highest contribution to the toll of Completely Damaged dwellings (figure 4.2).

The great majority of dwellings in masonry structures belong to buildings with 1 or 2 floors (table 3.3) which have a natural frequency similar to the average frequency of intermediate soils. This causes a resonance effect, originating the observed dominant damage in intermediate soils.

4.2. Human losses

The pattern of human losses reveals that most casualties occur in the *Adobe and rubble stone* typological class. This is a consequence of the death rate assigned to this class, which was used in the human loss model. In fact, the default values rates proposed by FEMA & NIBS [1999] were calibrated by Portuguese historical earthquakes (1755, 1909 and 1969) [Sousa, 2006]. The calibration process could induce some bias, because *RC* building stock could only be assessed in the low intensity 1969 earthquake (2 deaths).

4.3. Economic losses

Figure 3.7 showed that total constructed area [m^2] of *RC* typological classes largely prevail in MAL region at the date of 2001 Censos. In particular, between 1960 and 1985, a clear *RC* construction boom took place in this region leading to the highest incidence of this typological class. After 1985 building construction declined being however the second most important typological class in terms of dwelling area.

Nevertheless, for 475 years return period, lost area normalized by exposure in each typological and soil classes (figure 4.5) shows that *Masonry* structures located in *intermediate soil* are the most vulnerable typological classes.

An interesting feature is that although total area exposure shows an incidence increase from soft to hard soils (figure 3.7), lost area normalized by exposure inverts this tendency in RC buildings (figure 4.5). This is effect result from RC buildings having, in general, higher number of stories than masonry buildings, suffering with low frequency content of soft soils profiles.

Another interesting feature comes out from the analysis of figure 4.5: ductile RC buildings, constructed after 1986, appear to be as vulnerable as non-ductile RC buildings constructed before 85. A possible explanation for that contradictory observation is that although ductile RC structures shows less collapses (higher displacement capacity in Complete Damage state), the figures for Slight and Moderate Damages tend to be higher when compared to the corresponding values of the older non-ductile RC frames, due to the predictable larger displacements achieved in modern RC ductile structures.

When absolute figures of Lost Area are analyzed (figure 4.6), the old non-ductile RC buildings (1960-85) are responsible for the higher losses in construction area. However, those figures are a consequence of the high exposure of this typological class.

Figures 4.7 and 4.8 express, in monetary terms, the results already discussed for the Lost Area. Monetary losses are obtained multiplying lost area by a reconstruction cost per m², officially published in Portuguese law entitled *Portaria n° 1062-C/2000* of October, 31. This cost takes into account the importance of the region in which reconstruction activities are considered, showing a slight variation in MAL.

5. SEISMIC RISK CURVES

Sousa [2006] showed that the substitution of modal scenarios (similar to those derived by disaggregation analysis in section 2.2.1) into the original attenuation laws used to compute seismic hazard has the capability to reproduce the hazard target level with great accuracy. Furthermore, each target level is associated to an exceedance probability or return period. Consequently, the modal hazard scenarios derived by disaggregation analysis, and correspondent losses as well, are representative of those period return periods. These assumptions fundamentals the risk curves drawn in figures 5.1 to 5.3:

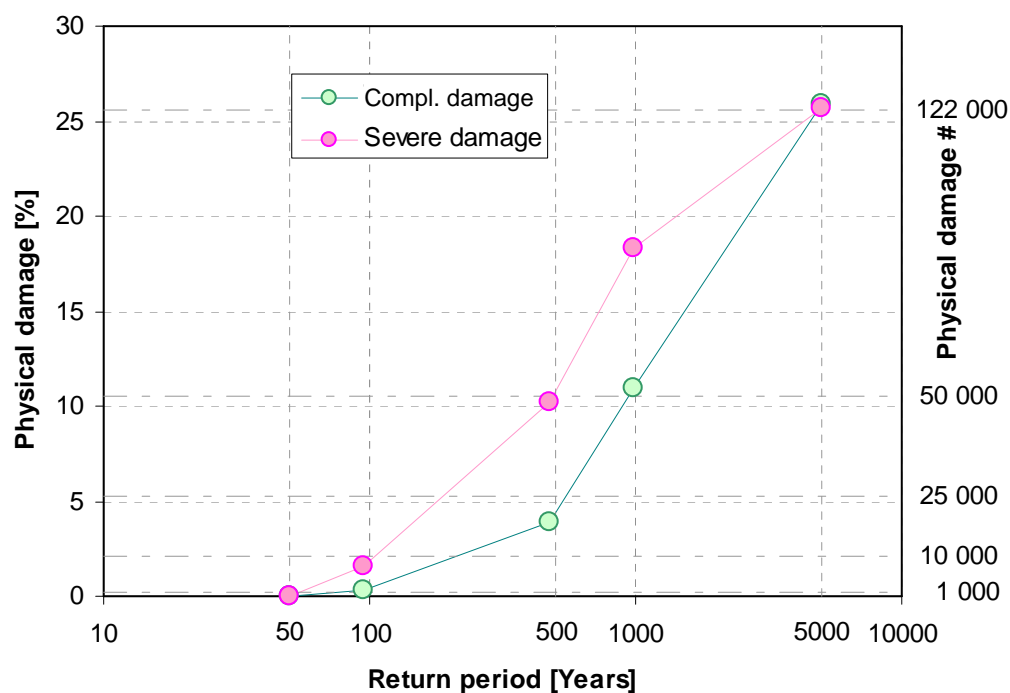


Figure 5.1 – Reference situation: seismic risk curves for physical damages in buildings.

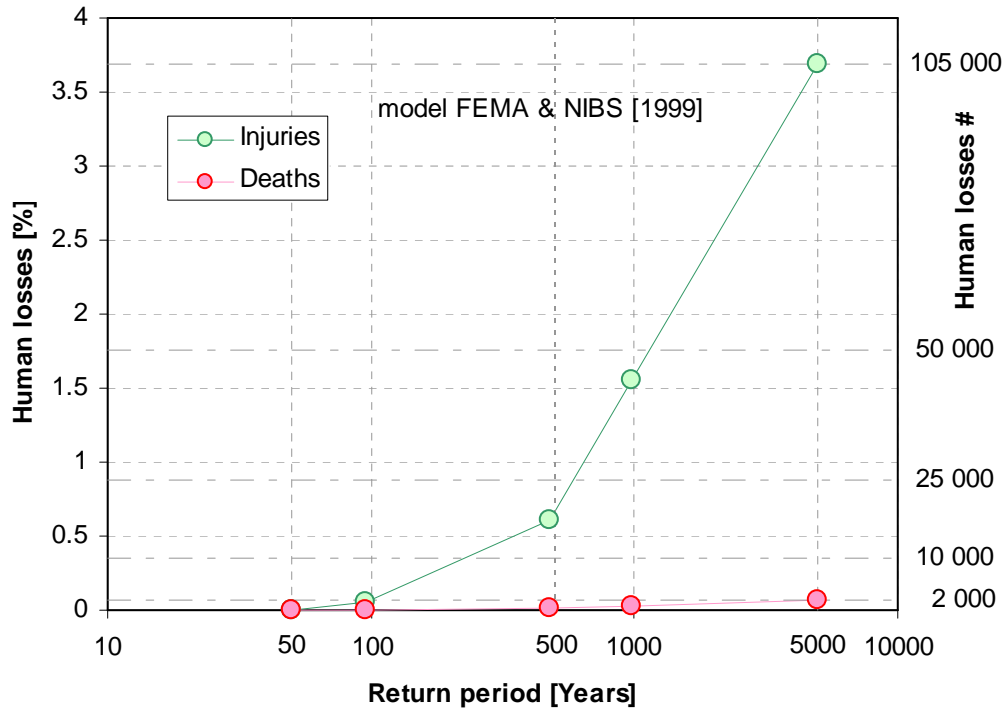


Figure 5.2 – Reference situation: seismic risk curves for human losses. FEMA & NIBS [1999] model.

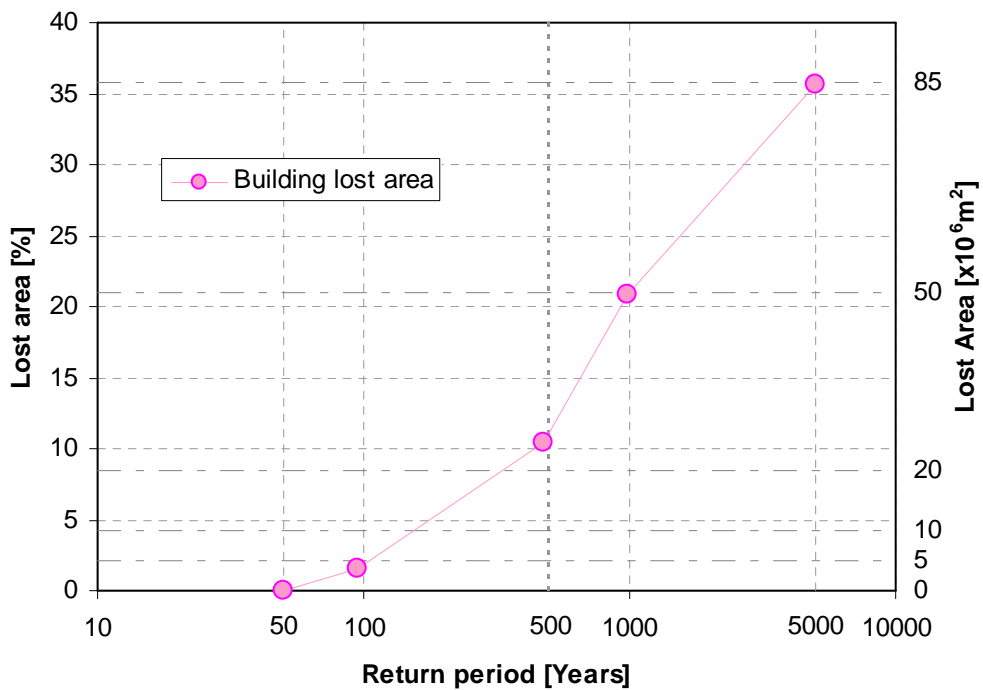


Figure 5.3 – Reference situation: seismic risk curves for economic losses measured in terms of percentual (left scale) and absolute (right scale) building lost area.

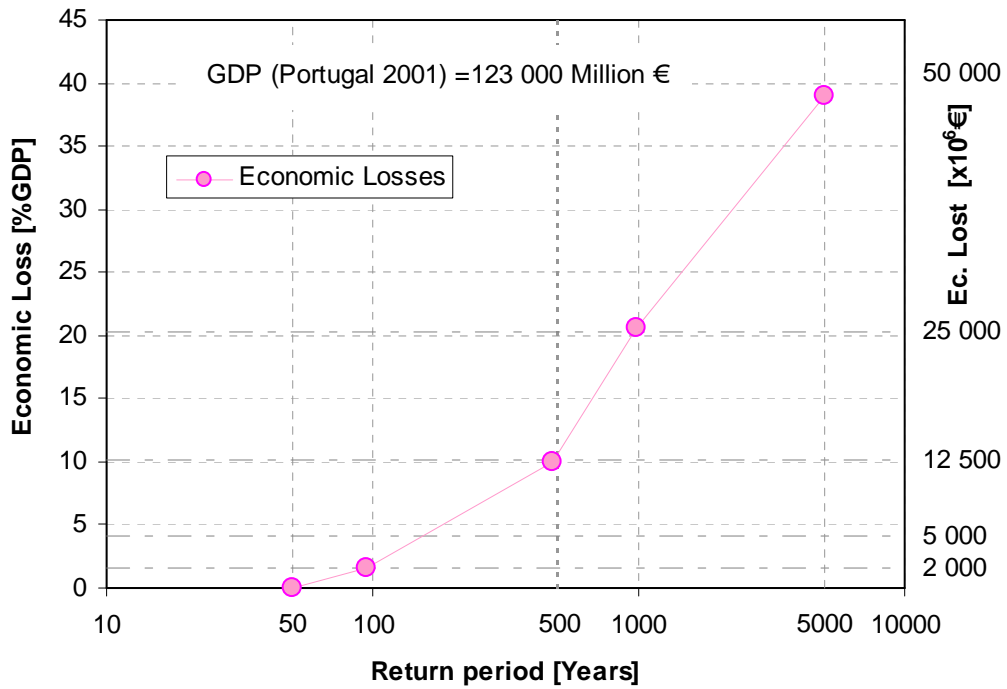


Figure 5.4 – Reference situation: seismic risk curves for economic losses measured in terms of absolute economic losses in millions of Euros (right scale) and as a percentage (left scale) of Portuguese GDP of 2001.

The analysis of those curves allows to conclude that there exists a major increase in losses with the return period growing, showing an inflexion point at the 475 return period (magnitude = 7.9).

6. FINAL CONSIDERATIONS

This report revised seismic ground motion scenarios relatively to the ones presented in deliverable 83, as a result of a great progress that took place in the last year in seismotectonic studies carried out in Portuguese seismic offshore region (see section 2.1). As a consequence higher values for seismic action levels for the same return periods were obtained, particularly concerning long distance offshore scenarios. Those further developments change the relative importance of short distance versus long distance scenarios on seismic input. In fact, from disaggregation analysis it was possible to conclude that seismic hazard in MAL is dominated by long distance scenarios, at least in what concerns return periods greater than 50 years.

The main purpose of chapter 3 is to present the results for reference scenarios. In order to enhance the principal features influencing losses estimations, the results are presented in a condensed form. In fact, LNECloss algorithms are very detailed in the description of typologies (315) and soils conditions (37 soil profile units). Thus results were aggregated in 3 classes of ground types and 7 typological classes which turned out more comprehensive and facilitating posterior design of mitigation policies.

Chapter 3 also presents the maps of loss estimates computed for 50 and 475 years return period scenarios. As for the 50 years return period there were no significant losses, a detailed analysis of losses estimations was not considered for this return period. Nevertheless, it was decided to compute seismic risk curves for MAL region, extending the number of return periods and corresponding scenarios, to 95, 975 and 5000 years, additionally to the other two referred scenarios.

The main results for the reference scenarios presented in chapter 4 are repeated in this chapter in a tabulated form (tables 6.1 and 6.2).

Table 6.1 – Number of deaths in each typological and soil classes; 475 years return period.

<i>Ground type</i>	Adobe + rubble stone	Masonry ≤ 1960	Masonry 1961-85	Masonry 1986-01	RC ≤ 1960	RC 1961-85	RC 1986-01	Total
Hard	54	10	10	2	1	2	1	80
Interm.	67	27	31	8	4	8	5	149
Soft	21	7	5	2	1	3	2	40
Total	142	43	46	12	5	13	8	269

Table 6.2 – Lost area [$10^6 m^2$] per typological and soil classes; 475 years return period.

Ground type	Adobe + rubble stone	Masonry ≤ 1960	Masonry 1961-85	Masonry 1986-01	RC ≤ 1960	RC 1961-85	RC 1986-01	Total
Hard	1.5	1.2	1.4	0.5	0.3	1.5	1.0	7.5
Interm.	1.4	2.1	2.4	1.1	0.7	2.1	1.5	11.4
Soft	0.5	0.5	0.3	0.2	0.2	0.6	0.5	2.7
Total	3.4	3.8	4.1	1.8	1.2	4.2	3.1	21.6

In what concerns 475 years return period scenario, results for human loss estimations, in absolute terms, indicate that the mitigation analysis should be more valuable if applied to *Adobe + rubble stone* buildings, to *Masonry* buildings constructed *before 1985* located on *intermediate soils*, and in a less extent to *Masonry* buildings constructed *before 1985* located on *hard soils*. The loss modeling results for these ground type categories and typological classes are signed bold in these tables.

For the same return period, the results for economic loss estimates, in absolute terms, indicate that the mitigation analysis should be worthwhile if applied to *Masonry buildings before 1985* located on *hard and intermediate soils*, to *Masonry buildings between 1985 and 2001* located on *intermediate soils*, to *RC buildings* constructed between *1961 and 1985* located on *hard and intermediate soils* and to *RC buildings* constructed between *1986 and 2001* located on *hard and intermediate soils*. Those analyses will be performed to accomplish deliverable 115.

7. REFERENCES

Bazzurro, P. [1998].

“Probabilistic seismic demand analysis”, PhD thesis, Stanford University.

Bazzurro, P. and Cornell, C.A. [1999].

“Disaggregation of seismic hazard”, *BSSA*, 89, 501-520.

Bernreuter, D.L. [1992]

Determining the controlling earthquake from probabilistic hazards for the proposed appendix B, *Lawrence Livermore National Laboratory*, Rep. UCRL-JC-111964, Livermore.

Calvi, G. M.; Pinho, R. [2004].

“LESSLOSS – A European Integrated Project on Risk Mitigation for Earthquakes and Landslides”. IUSS Press, Pavia.

Campos Costa, A., Sousa, M.L., Carvalho, A., Bilé Serra, J. and Carvalho, E.C. [2002],

“Regional seismic risk scenarios based on hazard deaggregation.”, Proceedings of the 12th European Conference on Earthquake Engineering, Paper 470.

Carvalho, E.C.; Campos Costa, A.; Sousa, M. L.; Martins, A.; Serra, J.B.; Caldeira. L.; Gomes Coelho, A. [2002].

“Caracterização, Vulnerabilidade e Estabelecimento de Danos para o Planeamento de Emergência sobre o Risco Sísmico na Área Metropolitana de Lisboa e nos Municípios de Benavente, Salvaterra de Magos, Cartaxo, Alenquer, Sobral de Monte Agraço, Arruda dos Vinhos e Torres Vedras. Contribuição para uma Simulação Simplificada de Danos. Relatório final“, Report280/02, G3ES, Proc. 037/1/13810, LNEC.

CEN, 2004.

“EN 1998-1. Eurocode 8: Design of structures for earthquake resistance – Part 1: General rules, seismic actions and rules for buildings”. Comité Européen de Normalisation. Bruxelles

Chapman, M.C. [1995]

“A probabilistic approach to ground-motion selection for engineering design”, *BSSA*, 85, 937-942.

Cramer, C.H. and Petersen, M.D. [1996]

“Predominant seismic source distance and magnitude maps for Los Angeles”, Orange and Ventura countries, California, *BSSA*, 86, 1645-1649.

Coburn, A.; Spence, R. [2002].

“Earthquake Protection”. Second Edition. John Wiley & Sons, 420 p.

FEMA & NIBS [1999].

“Earthquake Loss Estimation Methodology – HAZUS 99”, Federal Emergency Management Agency and National Institute of Buildings Sciences, Washington, D.C., USA.

Frankel, A., Mueller, C., Barnhard, T., Perkins, D., Leyendecker, E., Dickman, N., Hanson, S. and Hopper, M. [1996].

“National seismic-hazard maps: June 1996 documentation”, *U.S. Geological Survey*, Open-file report 96-532, <http://geohazards.cr.usgs.gov/eq/>.

Frankel, A., Mueller, C., Barnhard, T., Leyendecker, E., Wesson, R.L., Harmsen, S.C., Klein, F.W., Perkins, D.M., Dickman, N., Hanson, S.L. and Hopper, M.G. [2000].

“USGS national seismic hazard maps“, *Earthquake Spectra*, 16, nº1, 1-19.

Harmsen, S., Perkins, D. and Frankel, A. [1999].

“Deaggregation of probabilistic ground motions in the Central and Eastern United States“, *BSSA*, 89, 1-13.

INE [2002].

“Recenseamento da população e da habitação (Portugal) - Censos 2001“. Instituto Nacional de Estatística. Lisboa.

IPQ [2000].

“NP ENV 1998-1-1. Eurocódigo 8: Disposições para projecto de estruturas sísmo-resistentes. Parte 1-1: Regras gerais – acções sísmicas e requisitos gerais para as estruturas“ (in Portuguese).

Kramer, S.L. [1996].

“Geotechnical earthquake engineering“, Prentice-Hall series in Civil Eng. and Eng. Mechanics, New Jersey.

McGuire, R.K. [1995].

“Probabilistic seismic hazard analysis and design earthquakes: closing the loop“, *BSSA*, 85, 1275-1284.

Montilla, J.A. [2000].

“Agregación y desagregación de aceleraciones esperadas en la Península Ibérica utilizando sismicidad de fondo“, PhD thesis, Granada University.

Montilla J. A. P., Casado C. L., Romero J. H. [2002].

“Deaggregation in Magnitude, Distance, and Azimuth in the South and West of the Iberian Peninsula“, *Bull. Seism. Soc. Am.* 92

Motazedian, D. & Atkinson, G. [2005].

“Stochastic finite-fault modelling based on a Dynamic Corner Frequency“. *BSSA*, V. 95, 995-1010.

- Pinto, P.E., Giannini, R. and Franchin, P. [2004].
“Seismic reliability analysis of structures“, IUSS Press, Pavia.
- Sousa, M. L. [2006].
“Risco Sísmico em Portugal Continental“. PhD thesis, Instituto Superior Técnico, Universidade Técnica de Lisboa, Portugal.
- Sousa, M.L.; Carvalho, A. [2001].
“Estudo de casualidade sísmica no Grupo Central do Arquipélago dos Açores“, Relatório 208/01, LNEC, Lisboa.
- Sousa, M.L., Carvalho, A. and Campos Costa, A. [2001].
“Seismic hazard de-aggregation for the Central Group of Azores Islands“, *Proceedings of the 5ESES*, LREC, Ponta Delgada. pp. 241-250.
- Sousa; M.L.; Campos Costa, A. [2006].
“Seismic Hazard Disaggregation Studies. Application to Mainland Portugal“. Paper nº 623, Proceedings 1st European Conference on Earthquake Engineering and Seismology, Geneva, Switzerland.
- Sousa, M.L; Oliveira, C.S. [1997].
“Hazard assessment based on macroseismic data considering the influence of geological conditions.“, *Natural Hazards*, 14, 207-225, Kluwer Academic Publishers.
- Vales, D., Fitas, A., Oliveira, C.S., Senos, L., Ramalheite, D., Carrilho, F. [1998].
“Atenuação inelástica para o norte e centro de Portugal,“ 1º Simp. APMG (in portuguese).
- UCAM, INGV, LNEC and AUTH teams [2005].
“Deliverable 83 – Technical report on the scenario earthquake definitions for three cities“. Report of SP10 project, for the project Lessloss Risk Mitigation for Earthquakes and Landslides, No.: GOCE-CT-2003-505488
- Wells, D.L., Coppersmith, K.J. [1994].
“New empirical relationships among magnitude, rupture length, rupture width, rupture area, and surface displacement.“ *Bull. Seism. Soc. Am.*, 84, pp. 974-1002.

8. ACKNOWLEDGEMENTS

The authors are very thankful to Dra. Anabela Martins that provided computation support to development of this report.

VISAS

Head of Earthquake Engineering and
Structural Dynamics Division



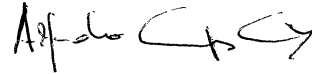
Ema Coelho

The Director of
Structures Department



João Almeida Fernandes

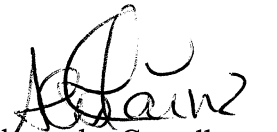
AUTHORS



Alfredo Campos Costa
Senior Research Officer



Maria Luísa Sousa
Research Officer



Alexandra Carvalho
Research Trainee

